Heavy Quarkonium Spectroscopy with PANDA

FAIR, May 2022

Johan Messchendorp (GSI, Darmstadt) on behalf of PANDA, QWG2022, September 30, 2022

Heavy Quarkonium Spectroscopy with PANDA

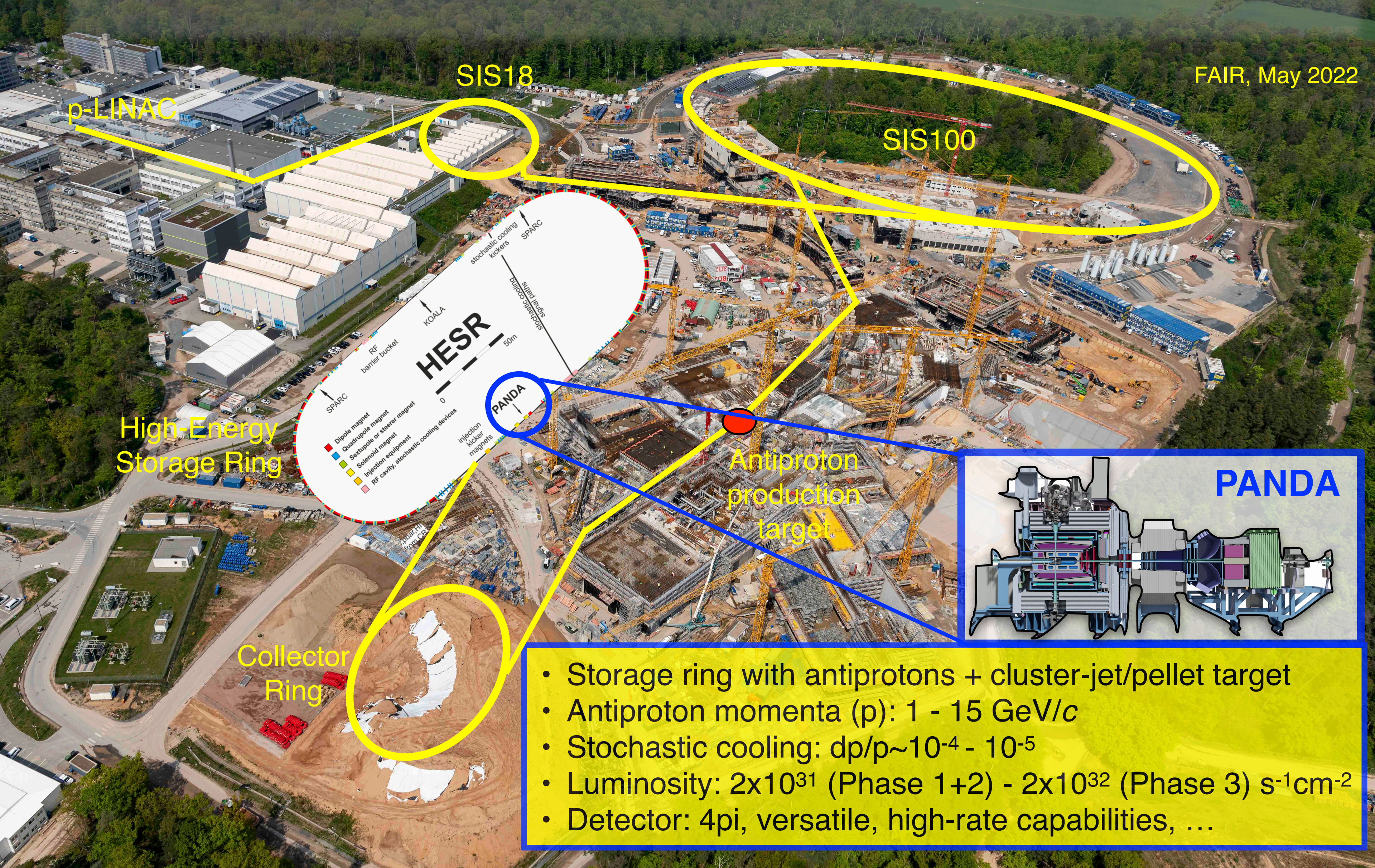

- Storage ring with antiprotons + cluster-jet/pellet target
- Antiproton momenta (p): 1 - 15 GeV/*c*
- Stochastic cooling: dp/p~10^{-4} - 10^{-5}
- Luminosity: 2×10^{31} (Phase 1+2) - 2×10^{32} (Phase 3) $s^{-1}cm^{-2}$
- Detector: 4pi, versatile, high-rate capabilities, …

Why antiprotons?

PANDA Phase One, EPJA57, 44 (2021)

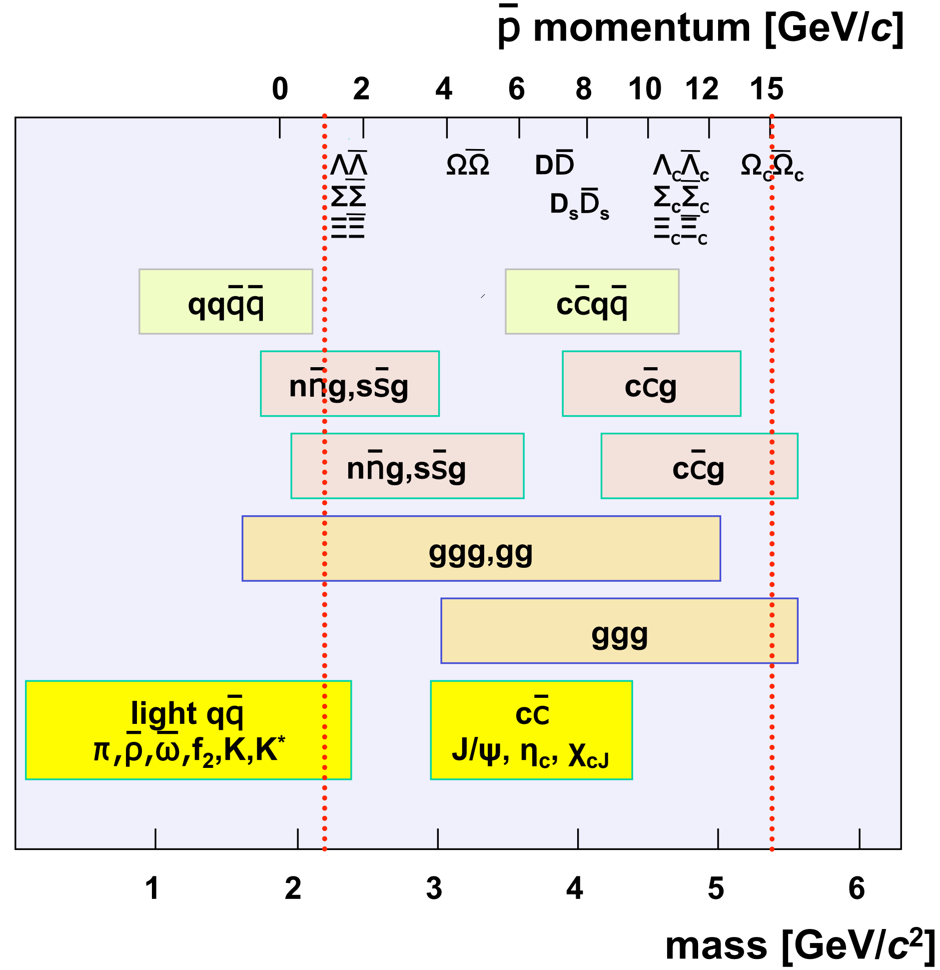

Why antiprotons?

PANDA Phase One, EPJA57, 44 (2021)

Large mass-scale coverage
- from light, strange, to charm-rich hadrons
- from quark/gluons to hadronic degrees of freedom

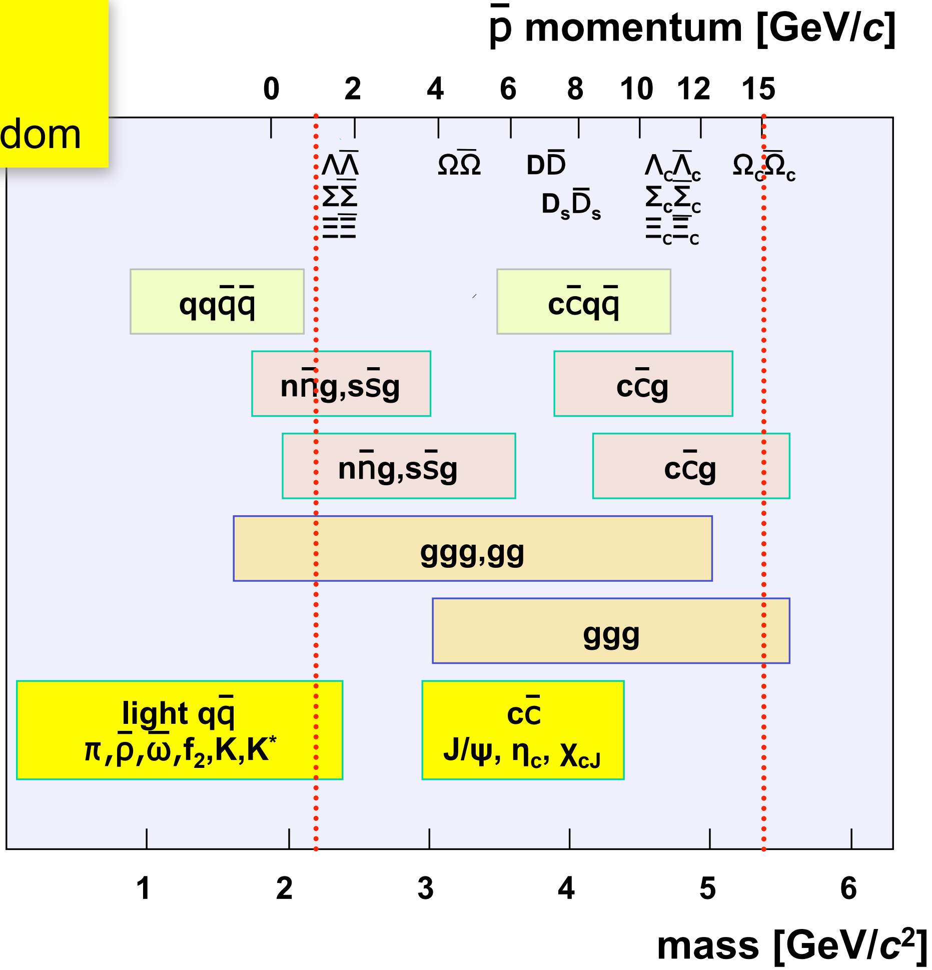

Why antiprotons?

PANDA Phase One, EPJA57, 44 (2021)

Large mass-scale coverage
- from light, strange, to charm-rich hadrons
- from quark/gluons to hadronic degrees of freedom

Large production rates of (exotic) hadrons
- charm+strange factory -> charmonium, hyperons!
- gluon-rich production -> potential for glueballs!

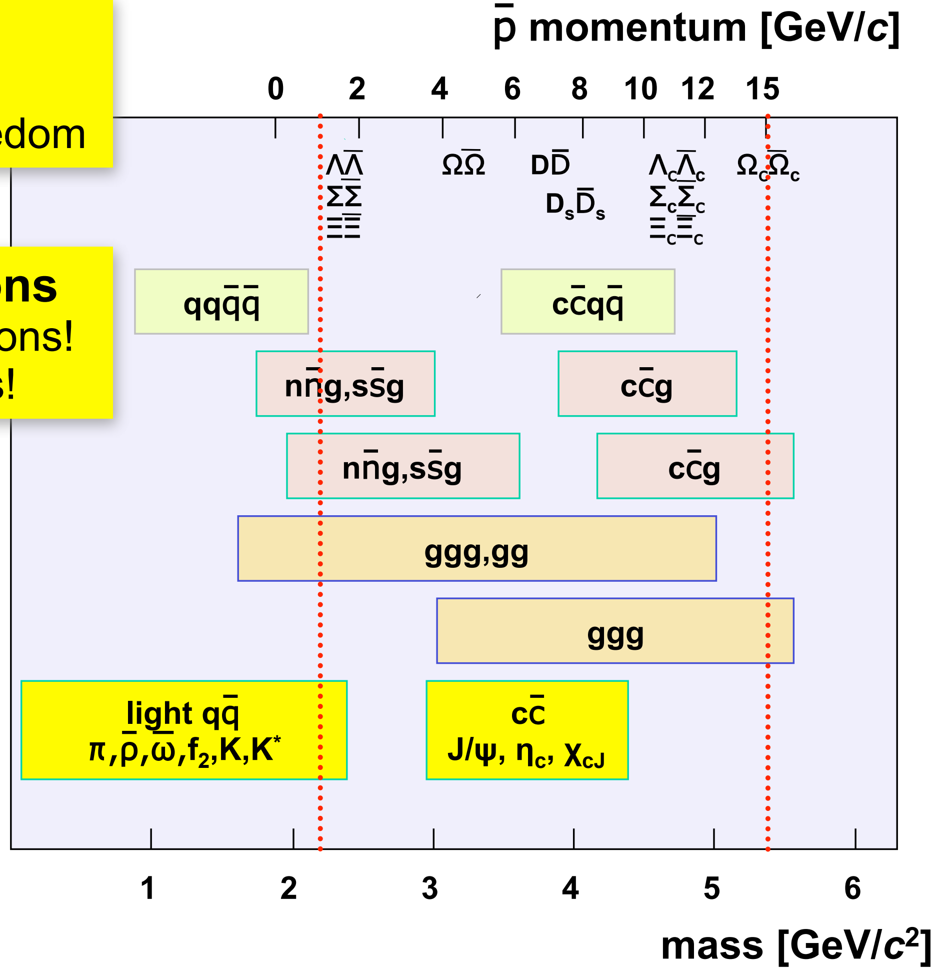

Why antiprotons?

PANDA Phase One, EPJA57, 44 (2021)

Large mass-scale coverage
- from light, strange, to charm-rich hadrons
- from quark/gluons to hadronic degrees of freedom

Large production rates of (exotic) hadrons
- charm+strange factory -> charmonium, hyperons!
- gluon-rich production -> potential for glueballs!

Access huge spectrum of hadrons
- direct formation of *all* conventional J^{PC} states
- large sensitivity to high spin states

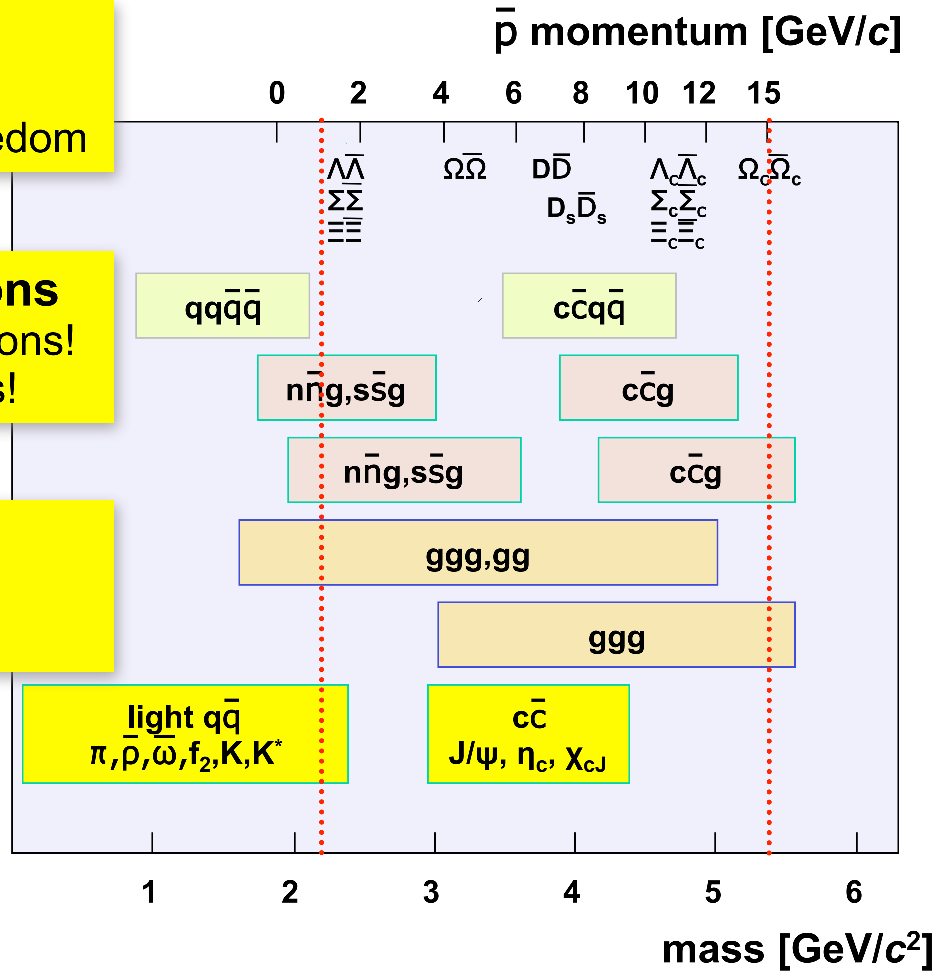

Why antiprotons?

PANDA Phase One, EPJA57, 44 (2021)

Large mass-scale coverage
- from light, strange, to charm-rich hadrons
- from quark/gluons to hadronic degrees of freedom

Large production rates of (exotic) hadrons
- charm+strange factory -> charmonium, hyperons!
- gluon-rich production -> potential for glueballs!

Access huge spectrum of hadrons
- direct formation of *all* conventional J^{PC} states
- large sensitivity to high spin states

Production of pairs of hadron+antihadrons
- matter-antimatter asymmetry studies
- excellent experimental conditions

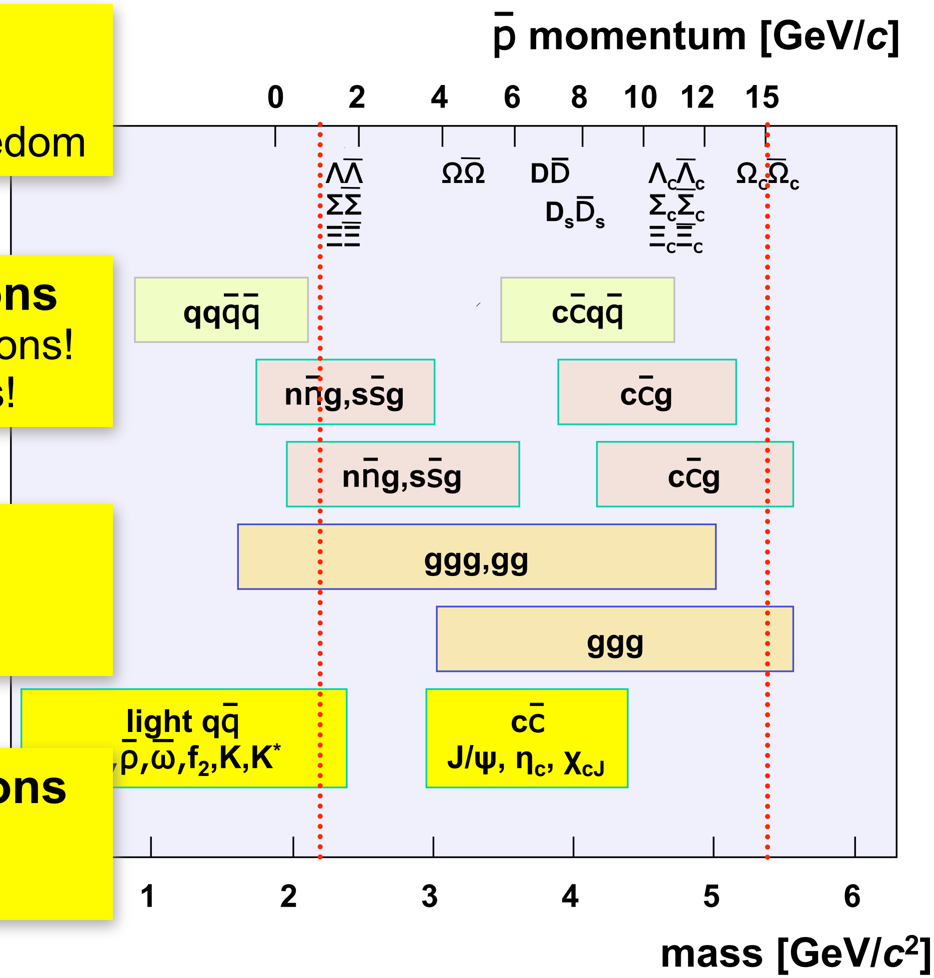

Why antiprotons?

PANDA Phase One, EPJA57, 44 (2021)

Large mass-scale coverage
- from light, strange, to charm-rich hadrons
- from quark/gluons to hadronic degrees of freedom

Large production rates of (exotic) hadrons
- charm+strange factory -> charmonium, hyperons!
- gluon-rich production -> potential for glueballs!

Access huge spectrum of hadrons
- direct formation of *all* conventional J^{PC} states
- large sensitivity to high spin states

Production of pairs of hadron+antihadrons
- matter-antimatter asymmetry studies
- excellent experimental conditions

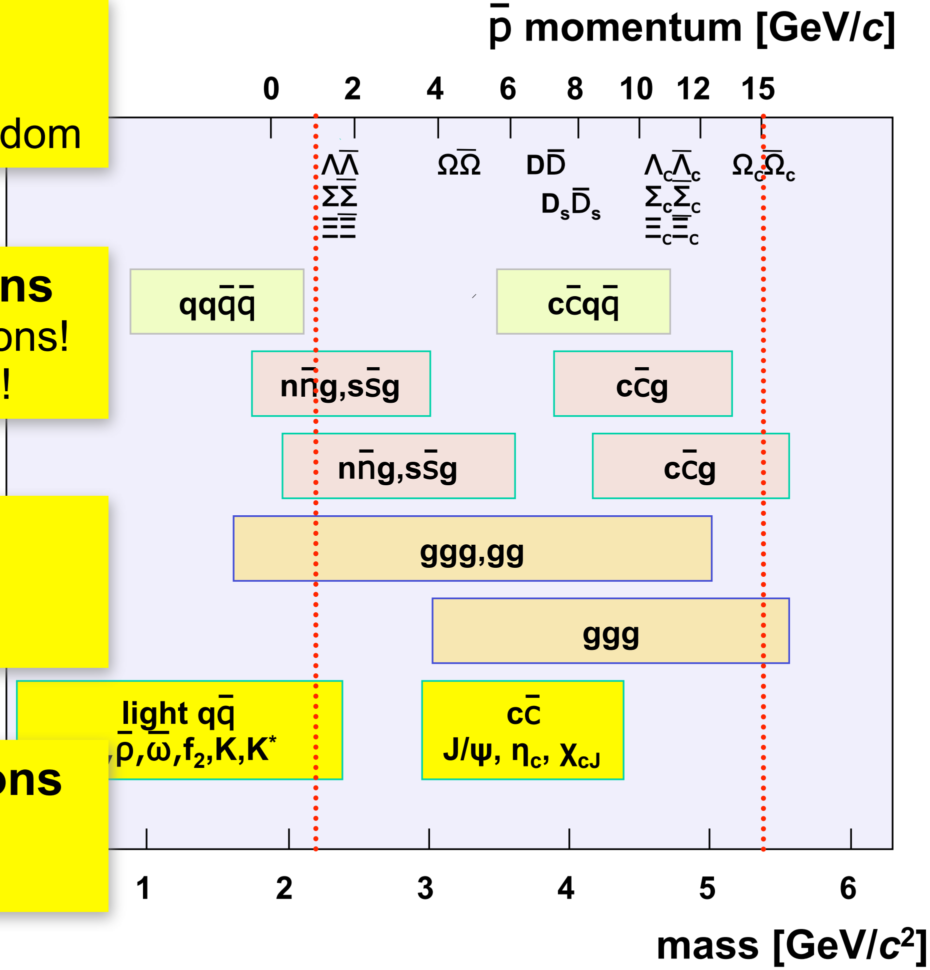

Unprecedented tool to rigorously study non-perturbative QCD!

PANDA physics overview

PANDA Phase One, EPJA57, 44 (2021)

Bound States and Dynamics of QCD

PANDA physics overview

PANDA Phase One, EPJA57, 44 (2021)

CHARM

STRANGE

LIGHT

Bound States and Dynamics of QCD

PANDA physics overview

PANDA Phase One, EPJA57, 44 (2021)

CHARM — **STRANGE** — **LIGHT**

BESIII, COMPASS, EIC, JLAB, ...

Nucleon Structure

Generalized Parton Distributions

Transition Distribution Amplitudes

Time-like Form Factors

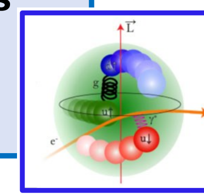

Bound States and Dynamics of QCD

PANDA physics overview

PANDA Phase One, EPJA57, 44 (2021)

CHARM — **STRANGE** — **LIGHT**

BELLEII, BESIII, COMPASS, JLAB, LHCb, ...

Spectroscopy

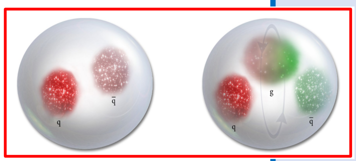

Hidden/open-charm states

Gluon-rich QCD states

Light-meson systems

BESIII, COMPASS, EIC, JLAB, ...

Nucleon Structure

Generalized Parton Distributions

Transition Distribution Amplitudes

Time-like Form Factors

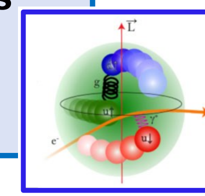

Bound States and Dynamics of QCD

PANDA physics overview

PANDA Phase One, EPJA57, 44 (2021)

CHARM — **STRANGE** — **LIGHT**

BELLEII, BESIII, COMPASS, JLAB, LHCb, …

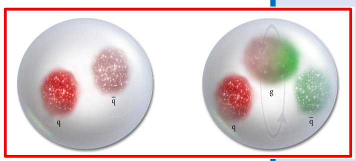

Spectroscopy

Hidden/open-charm states

Gluon-rich QCD states

Light-meson systems

BESIII, COMPASS, EIC, JLAB, …

Nucleon Structure

Generalized Parton Distributions

Transition Distribution Amplitudes

Time-like Form Factors

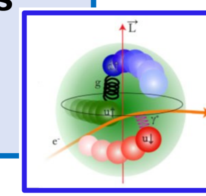

Bound States and Dynamics of QCD

Strangeness

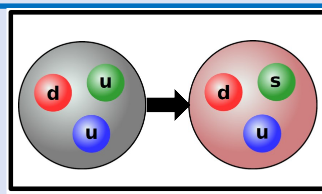

Strange baryon spectroscopy

Hyperon production & polarization

Hyperon transition form factors

BESIII, JLAB, JPARC, HADES, MAMI, ELSA, …

PANDA physics overview

PANDA Phase One, EPJA57, 44 (2021)

CHARM — **STRANGE** — **LIGHT**

BELLEII, BESIII, COMPASS, JLAB, LHCb, …

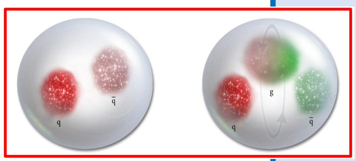

Spectroscopy

Hidden/open-charm states

Gluon-rich QCD states

Light-meson systems

BESIII, COMPASS, EIC, JLAB, …

Nucleon Structure

Generalized Parton Distributions

Transition Distribution Amplitudes

Time-like Form Factors

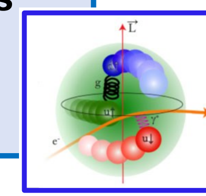

Bound States and Dynamics of QCD

Strangeness

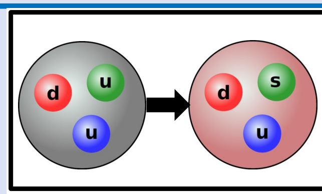

Strange baryon spectroscopy

Hyperon production & polarization

Hyperon transition form factors

BESIII, JLAB, JPARC, HADES, MAMI, ELSA, …

Nuclear Physics

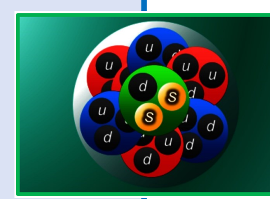

Hadrons in nuclei

Hyperon-nucleon dynamics

Hyper-atoms and nuclei

CBM, HYPHI, JPARC, …

PANDA physics overview

CHARM — **STRANGE** — **LIGHT**

BELLEII, BESIII, COMPASS, JLAB, LHCb, ...

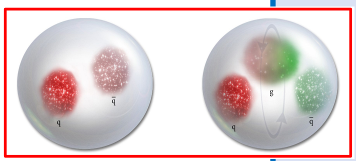

Spectroscopy

Hidden/open-charm states

Gluon-rich QCD states

Light-meson systems

BESIII, COMPASS, EIC, JLAB, ...

Nucleon Structure

Generalized Parton Distributions

Transition Distribution Amplitudes

Time-like Form Factors

Bound States and Dynamics of QCD

Strangeness

Strange baryon spectroscopy

Hyperon production & polarization

Hyperon transition form factors

BESIII, JLAB, JPARC, HADES, MAMI, ELSA, ...

Nuclear Physics

Hadrons in nuclei

Hyperon-nucleon dynamics

Hyper-atoms and nuclei

CBM, HYPHI, JPARC, ...

Charmonium-like particles - terra incognita

- Narrow states
- Heavy charm quarks

Charmonium-like particles - terra incognita

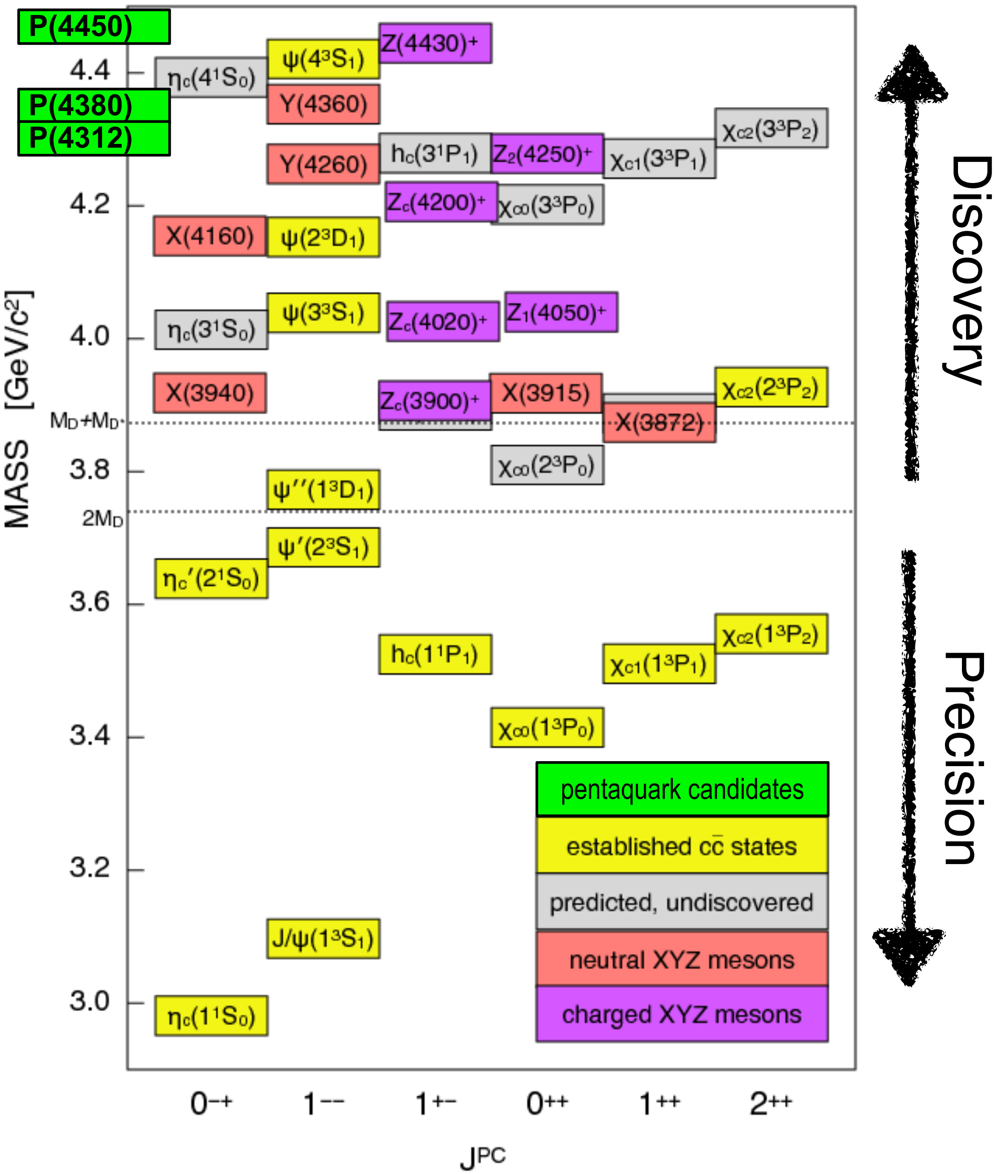

- Narrow states
- Heavy charm quarks

Charmonium-like particles - terra incognita

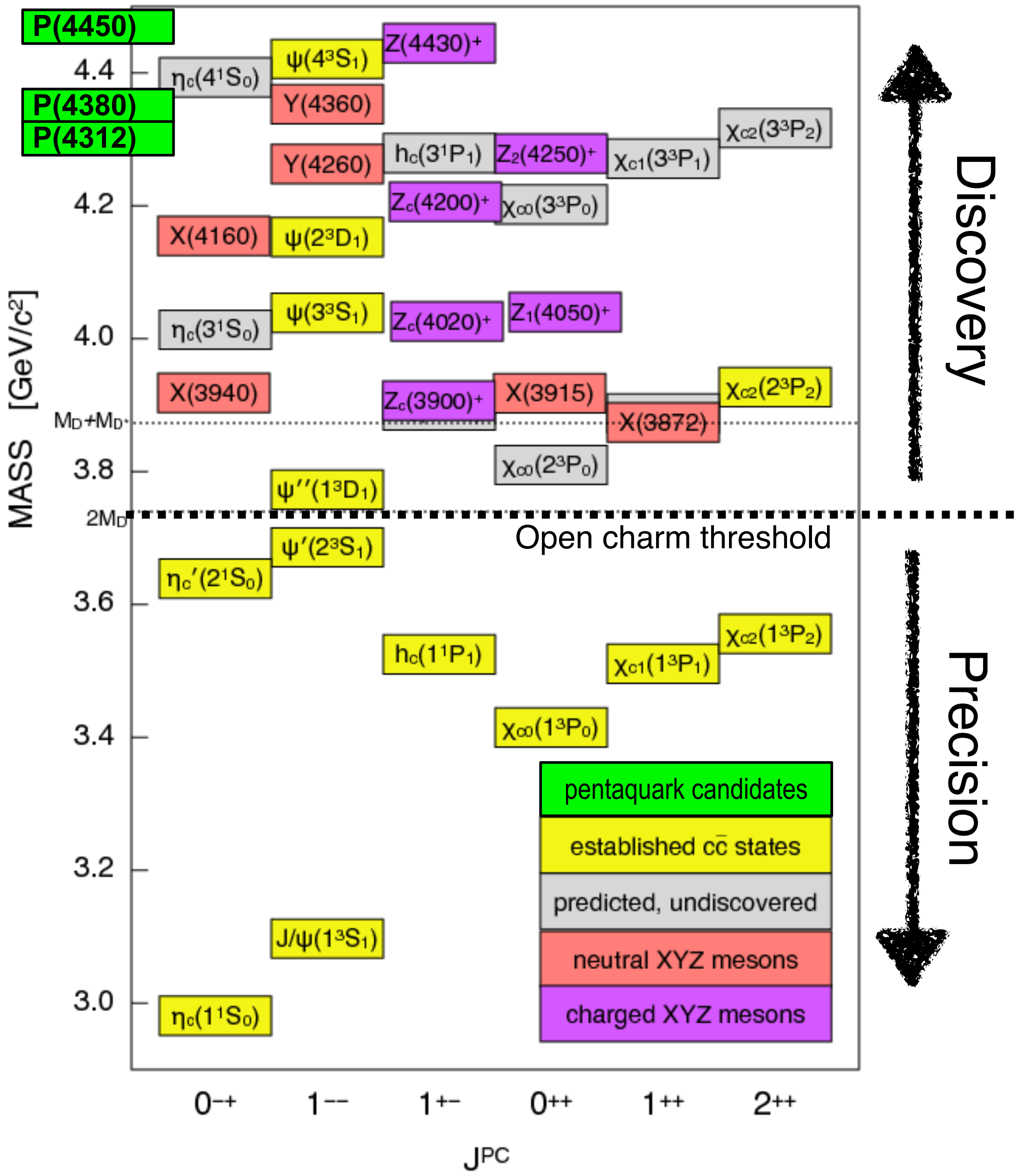

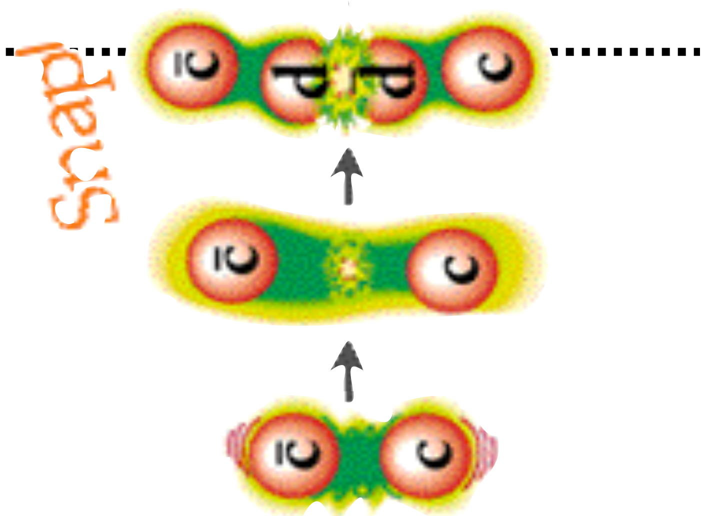

- Narrow states
- Heavy charm quarks

Charmonium-like particles - terra incognita

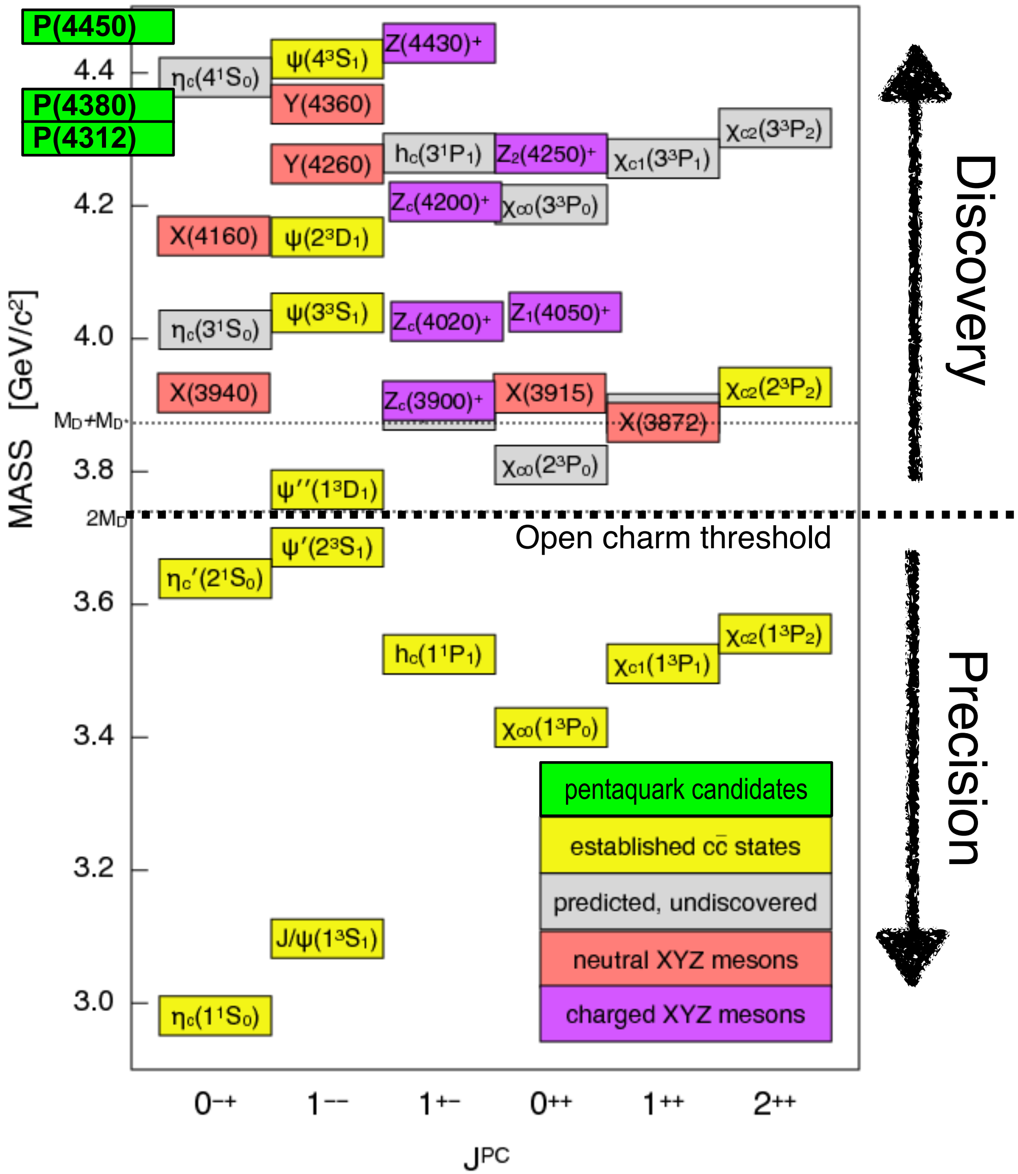

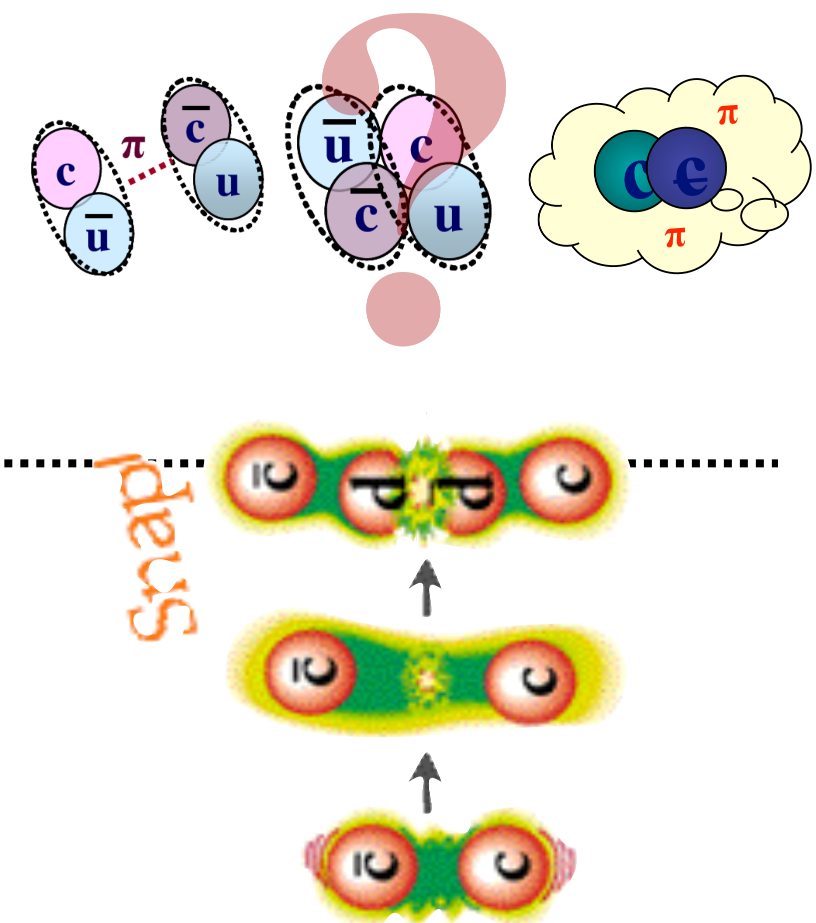

- Narrow states
- Heavy charm quarks

Charmonium-like particles - PANDA opportunities

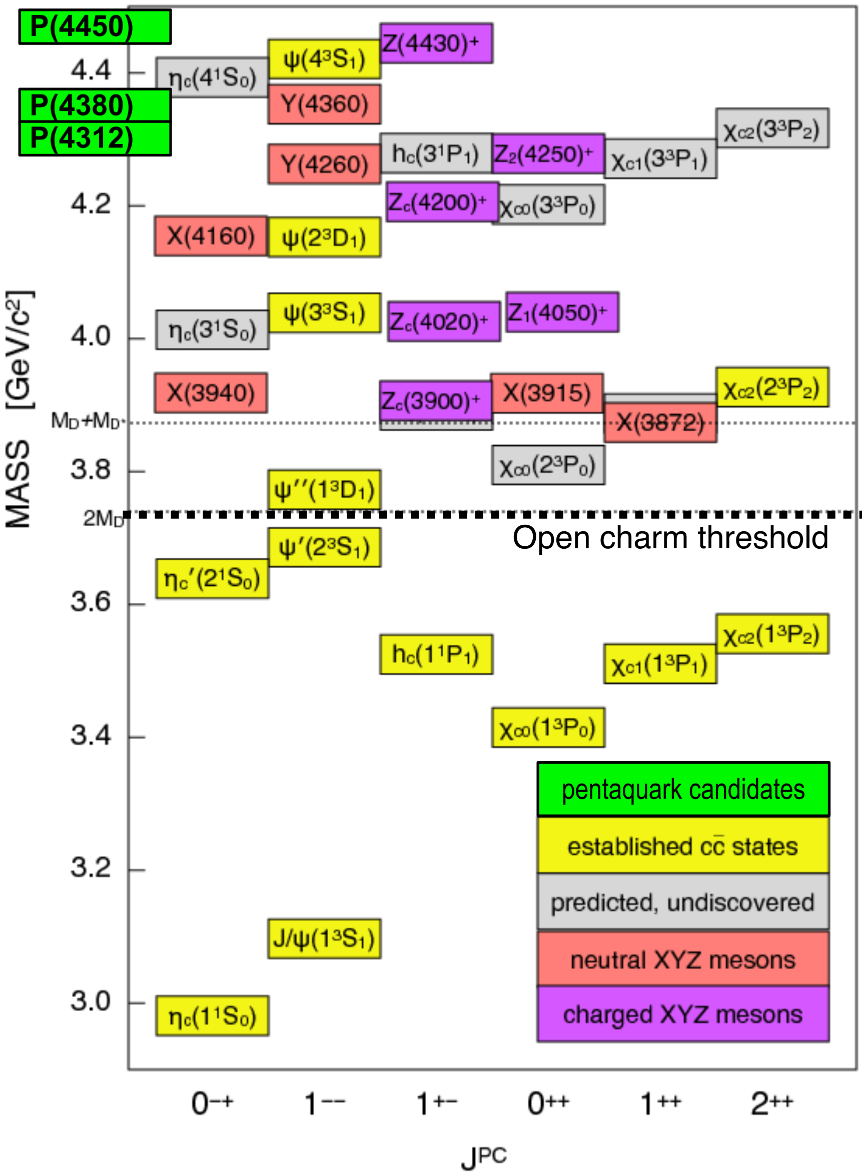

- line shape of, f.e., X(3872)
- neutral+charged Z-states
- X,Y,Z decays
- search for h_c', $^3F_4$, …
- spin-parity/mass&width of $^3D_2$
- Search for glueballs/hybrids

- line shape/width of the eta_c, h_c
- radiative transitions
- hadronic transitions
- light-quark spectroscopy

Charmonium-like particles - PANDA opportunities

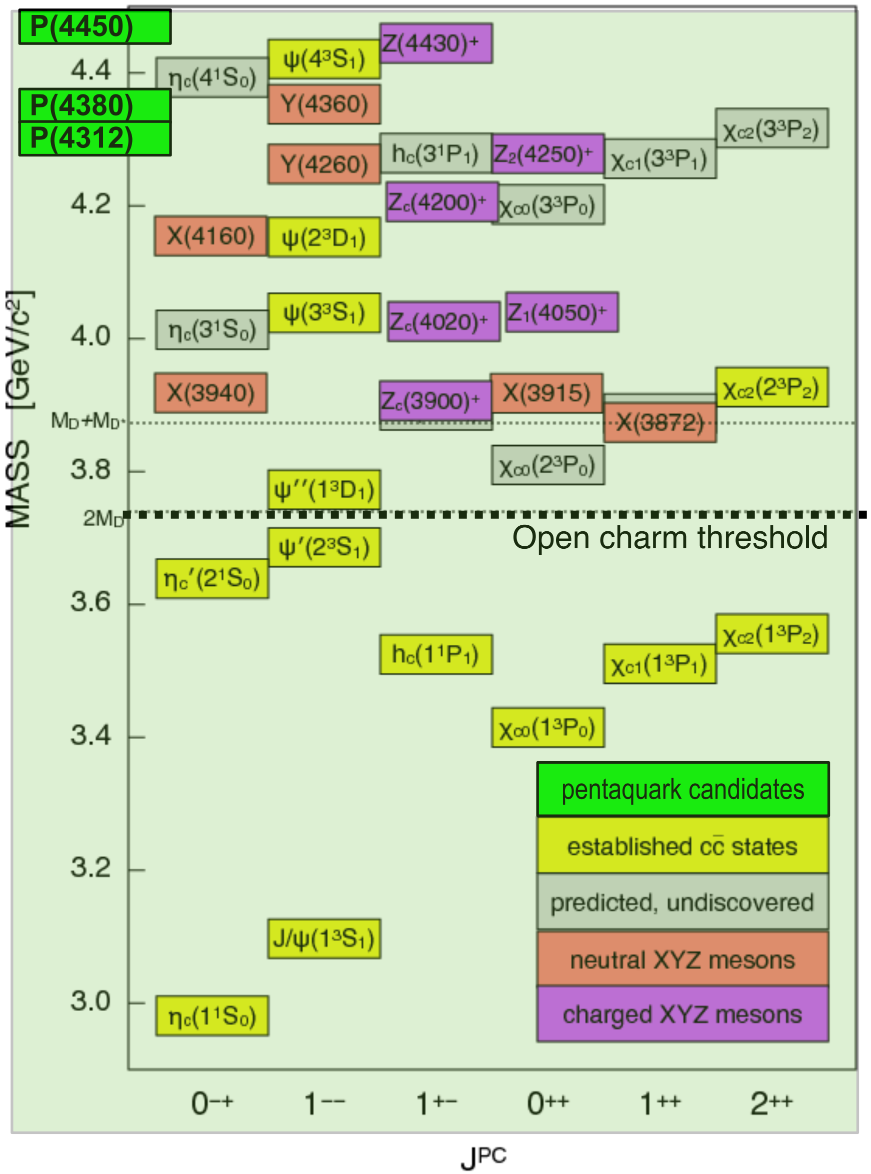

- line shape of, f.e., X(3872)
- neutral+charged Z-states
- X,Y,Z decays
- search for h_c', $^3F_4$, …
- spin-parity/mass&width of $^3D_2$
- Search for glueballs/hybrids

- line shape/width of the eta$_c$, h_c
- radiative transitions
- hadronic transitions
- light-quark spectroscopy

Charmonium-like particles - PANDA opportunities

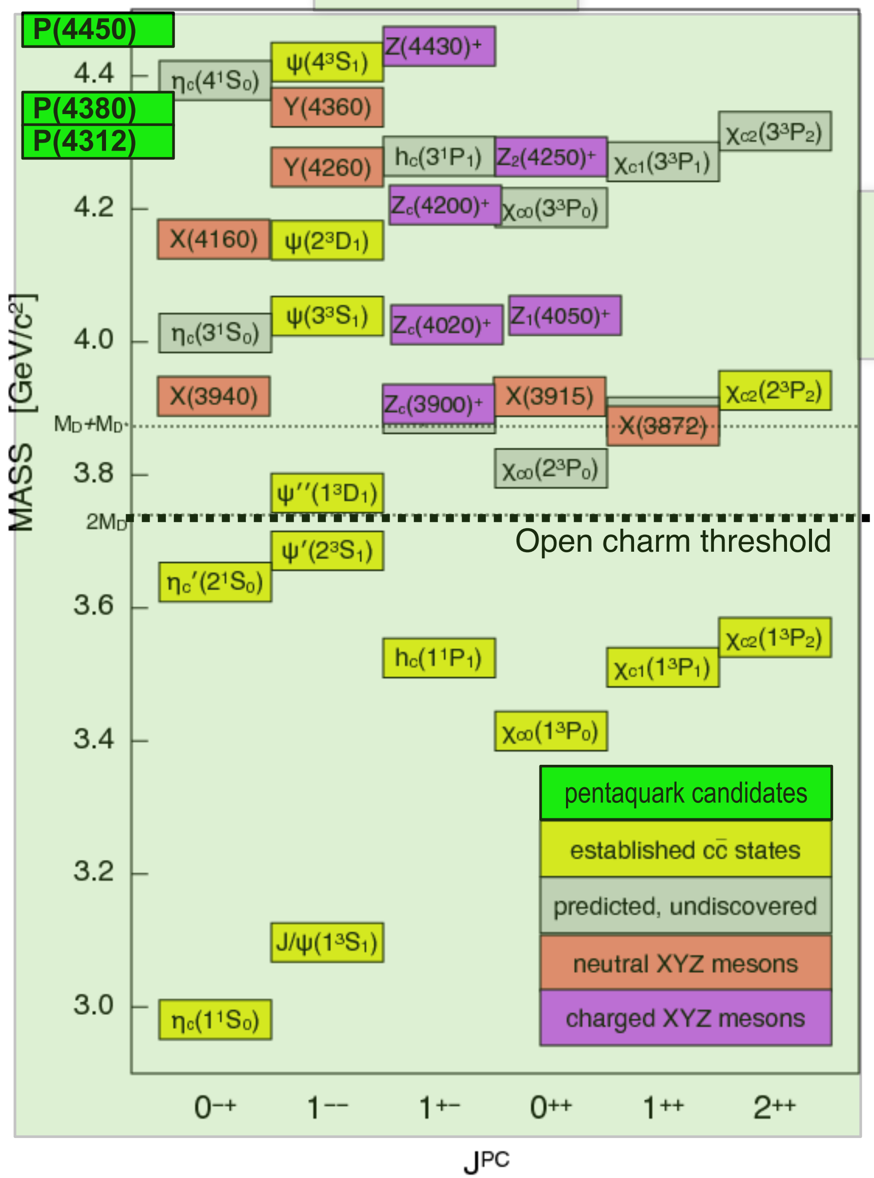

- line shape of, f.e., X(3872)
- neutral+charged Z-states
- X,Y,Z decays
- search for h_c', $^3F_4$, …
- spin-parity/mass&width of $^3D_2$
- Search for glueballs/hybrids

- line shape/width of the eta_c, h_c
- radiative transitions
- hadronic transitions
- light-quark spectroscopy

Charmonium-like particles - PANDA opportunities

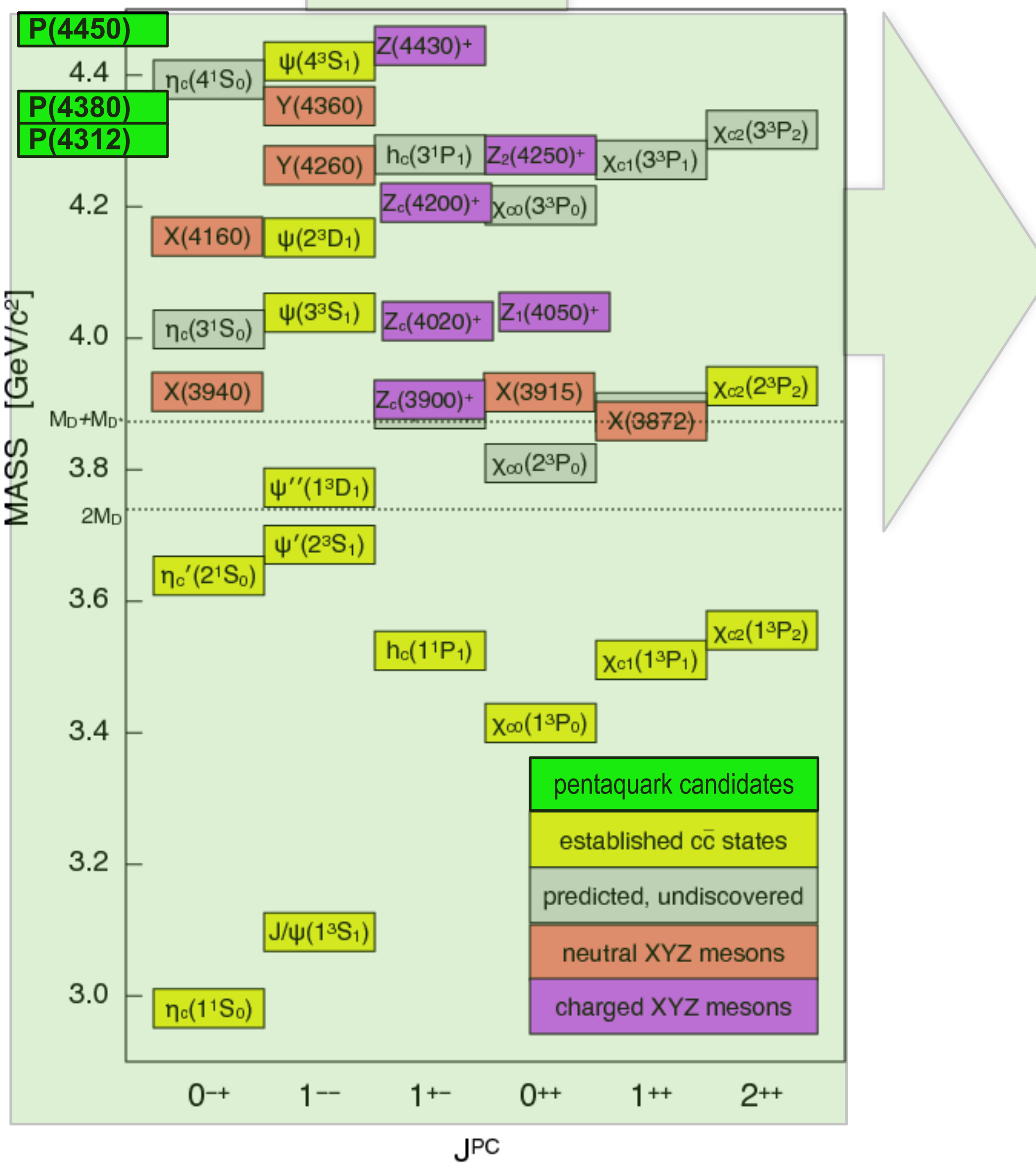

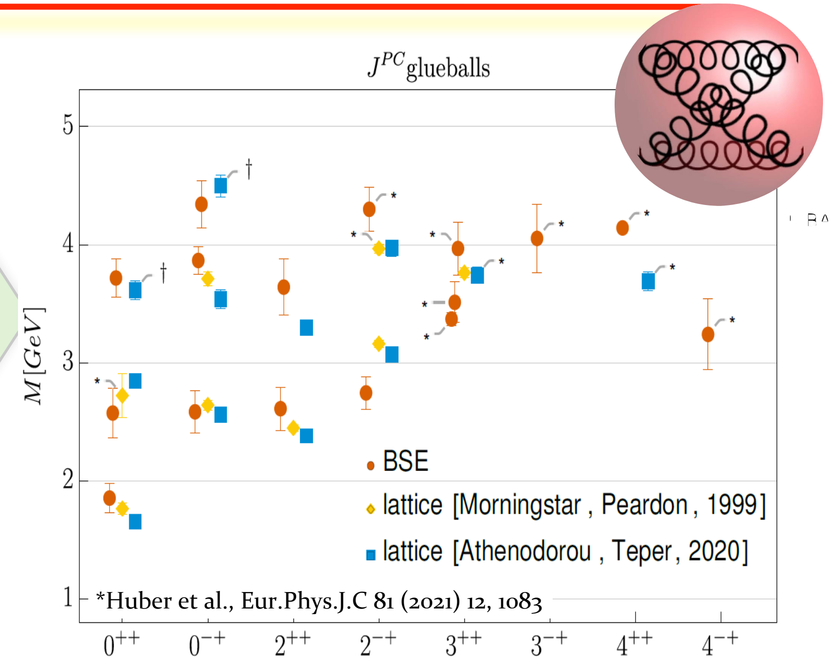

The X(3872)

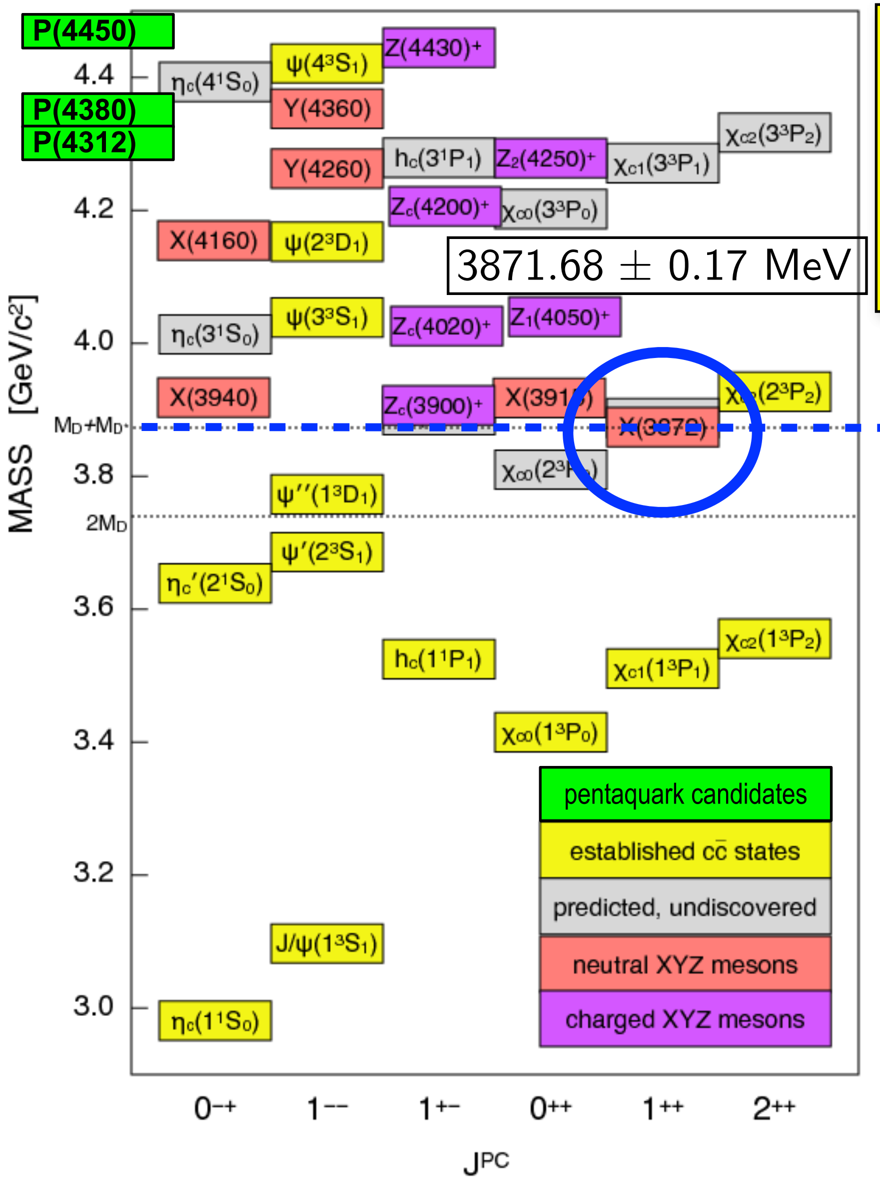

- **Close to DD* threshold**
- **Isospin breaking?**
- **Strikingly narrow**
- **Remains mysterious after decades**

➡Alternative insight needed!

The X(3872)

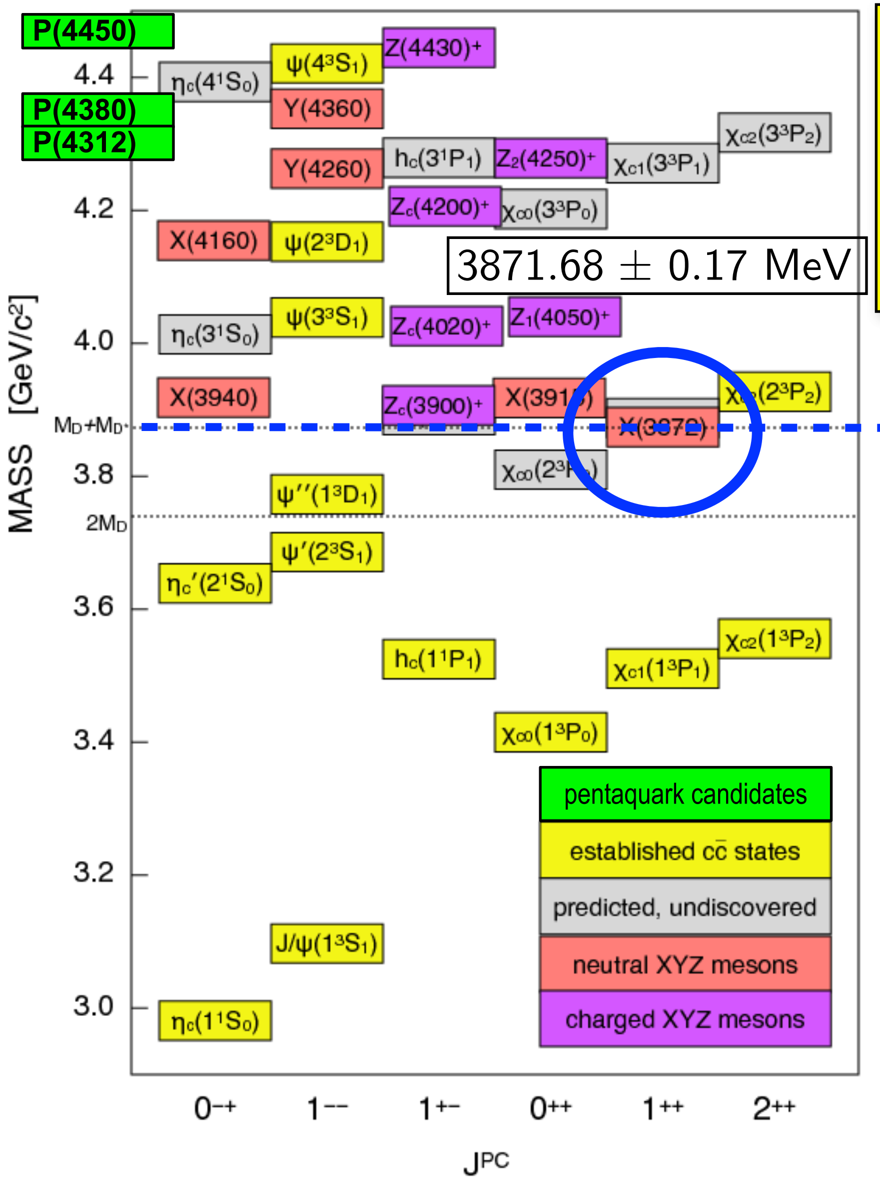

- **Close to DD* threshold**
- **Isospin breaking?**
- **Strikingly narrow**
- **Remains mysterious after decades**

➡Alternative insight needed!

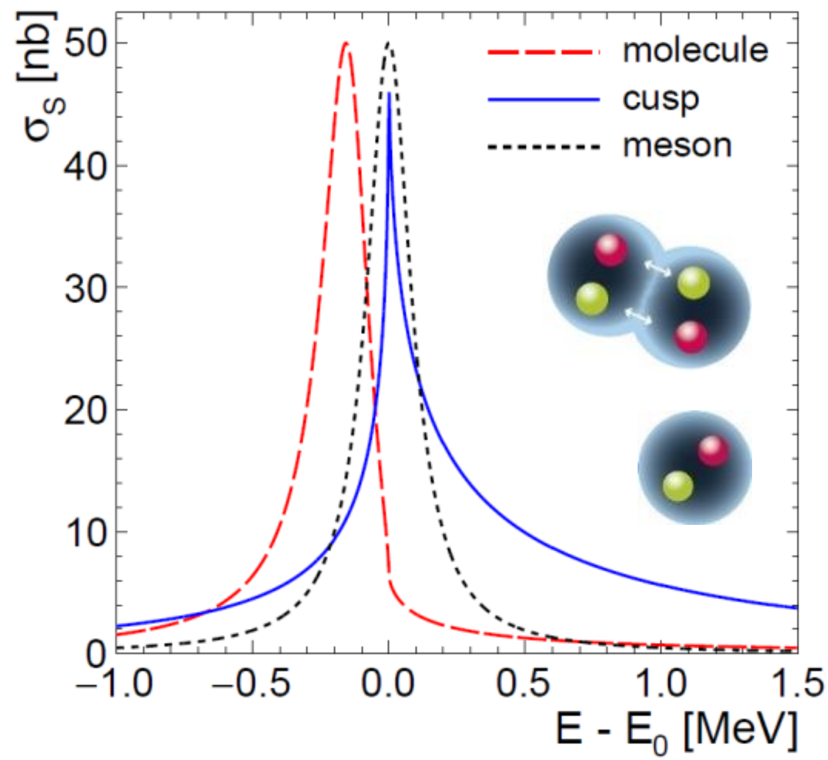

Line-shape of the X(3872)

- Different internal structure → different production/decay dynamics
- Idea: Line shape of resonance reveals nature!
- Challenge: High resolution needed to resolve structures!

[CDF, PRL 103 (2009) 152001]

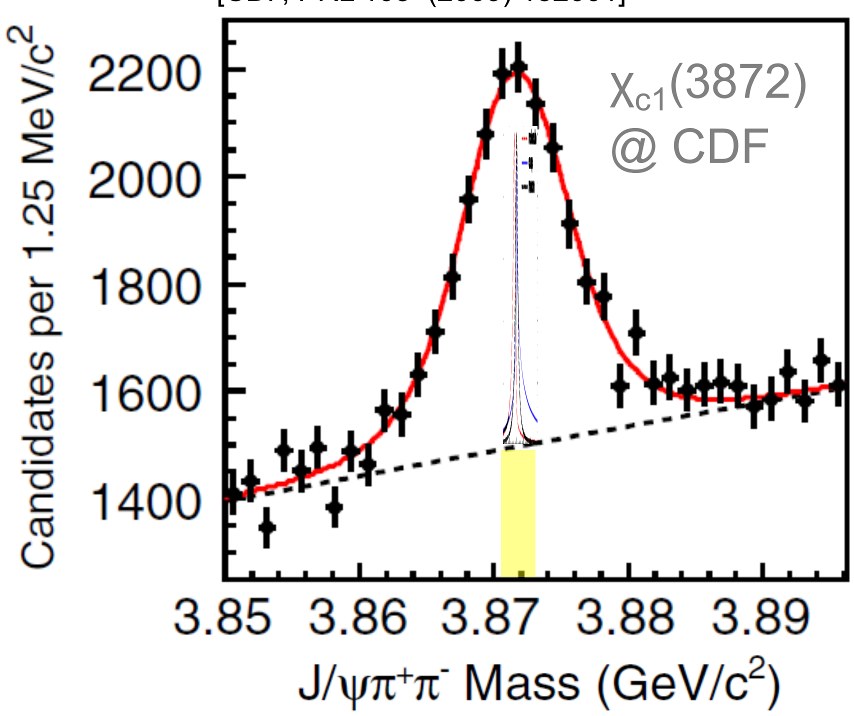

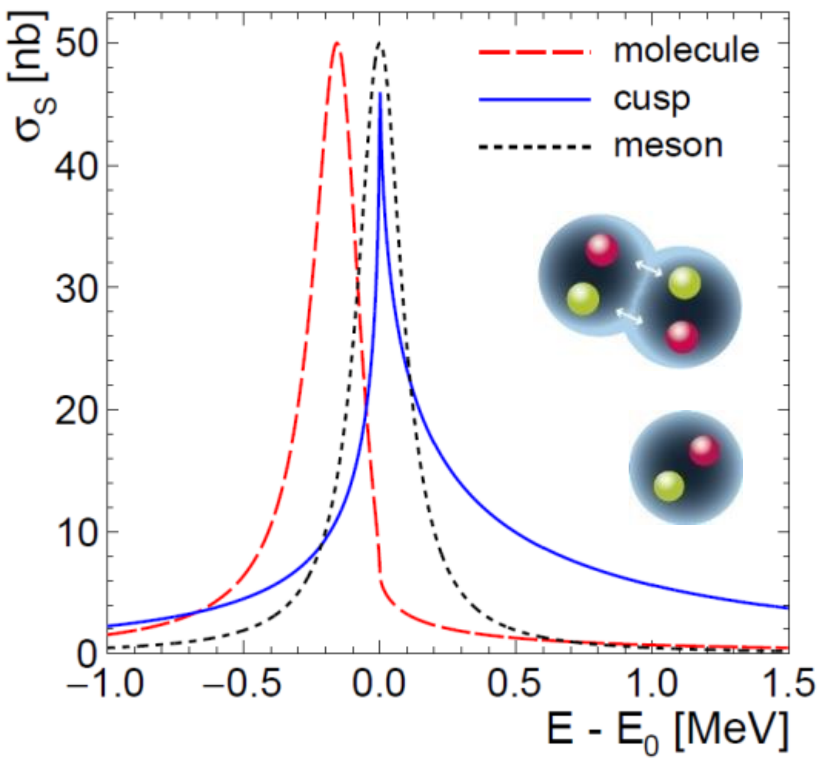

Resonance scanning

- Production with recoils dominated by detector resolution (~ MeV)
- Formation reaction → produce $\chi_{c1}(3872)$ [$J^{PC} = 1^{++}$] w/o recoils

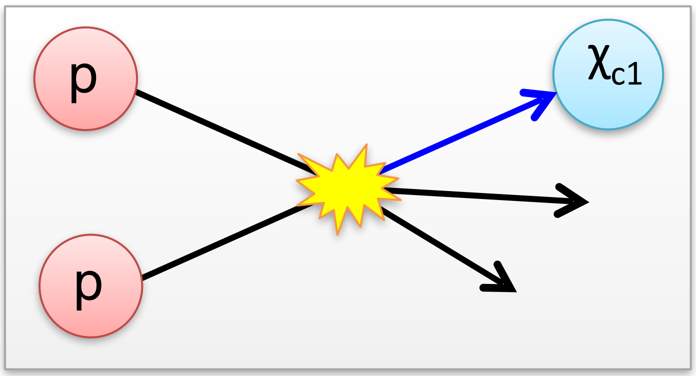

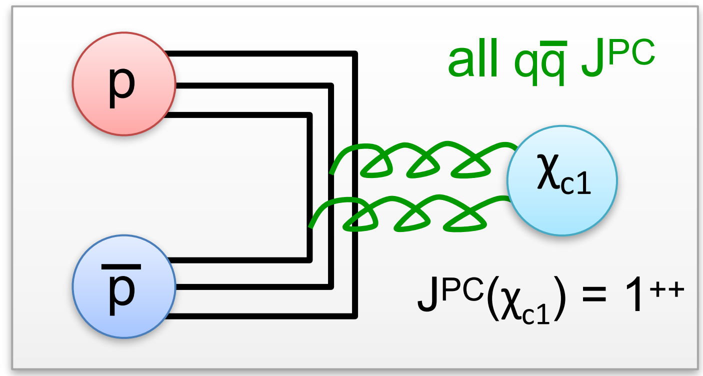

Resonance scanning

- Production with recoils dominated by detector resolution (~ MeV)
- Formation reaction → produce χ_{c1}(3872) [$J^{PC} = 1^{++}$] w/o recoils

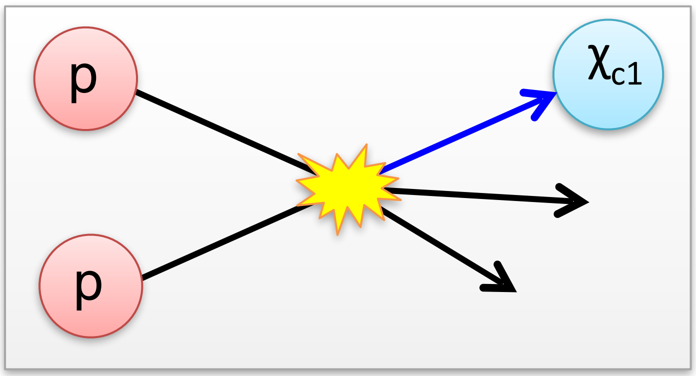

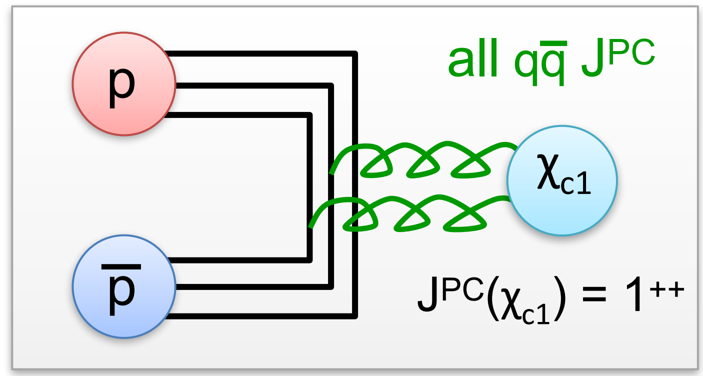

- Beam energy spread → resolution
- Measure yield at different E_{cms}

LHCb Detector Resolution ≈ 2.6 MeV
PANDA Beam Resolution ≈ 0.05 MeV

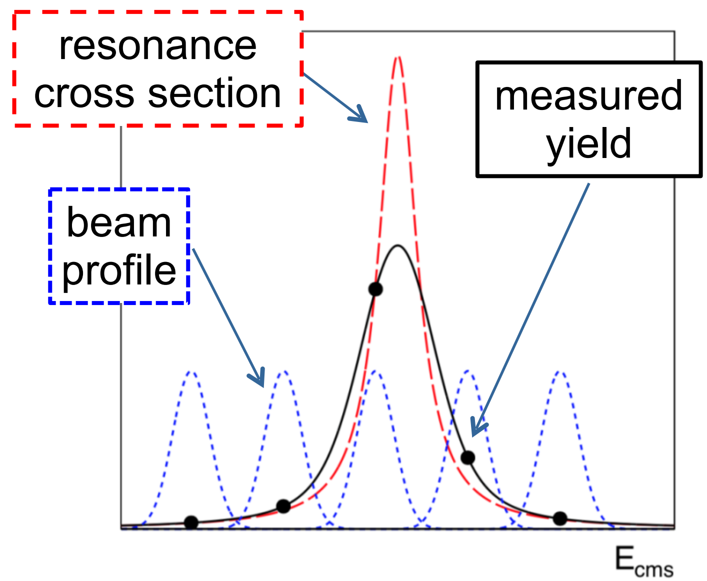

Comprehensive sensitivity study

Klaus Goetzen, Frank Nerling, et al.

Eur. Phys. J. A (2019) **55**: 42
DOI 10.1140/epja/i2019-12718-2 [https://arxiv.org/abs/1812.05132]

THE EUROPEAN PHYSICAL JOURNAL A

Regular Article – Experimental Physics

Precision resonance energy scans with the PANDA experiment at FAIR

Sensitivity study for width and line shape measurements of the X(3872)

- Reaction: $\bar{p}p \to \chi_{c1}(3872) \to J/\psi\ (\to e^+e^- / \mu^+\mu^-)\ \rho^0\ (\to \pi^+\pi^-)$
- Determine the precision for line-shape measurement at PANDA of
  - Breit-Wigner Width **Γ**
  - Flatté Energy $\mathbf{E_f}$
- Investigated Parameter Space:

Total beam time: $T = 40 \times 2d$ $= 80$ d

Cross section assumption: $\sigma_{peak}(\bar{p}p \to \chi_{c1})$ $= 20\ ..\ 150$ nb

BW Width: Γ = [50, 70, 100, 180, 250, 500] keV

Flatté energy: E_f = [-10.0, -9.5, -9.0, -8.8, -8.3, -8.0, -7.5, -7.0] MeV

Flatte model

Klaus Goetzen, Frank Nerling, et al.

- Line shapes for Flatté model [Hanhart et al, PRD 76 (2007) 034007]
- Channel: $\chi_{c1}(3872) \rightarrow J/\psi\ \rho^0$

$$\sigma\left(E; E_f\right) \sim \frac{\Gamma_{\pi^+\pi^- J/\psi}(E)}{|D(E; E_f)|^2}$$

$$D(E) = E - E_f + \frac{i}{2}[g(k_1 + k_2) + \Gamma_\rho(E) + \Gamma_\omega(E) + \Gamma_0]$$

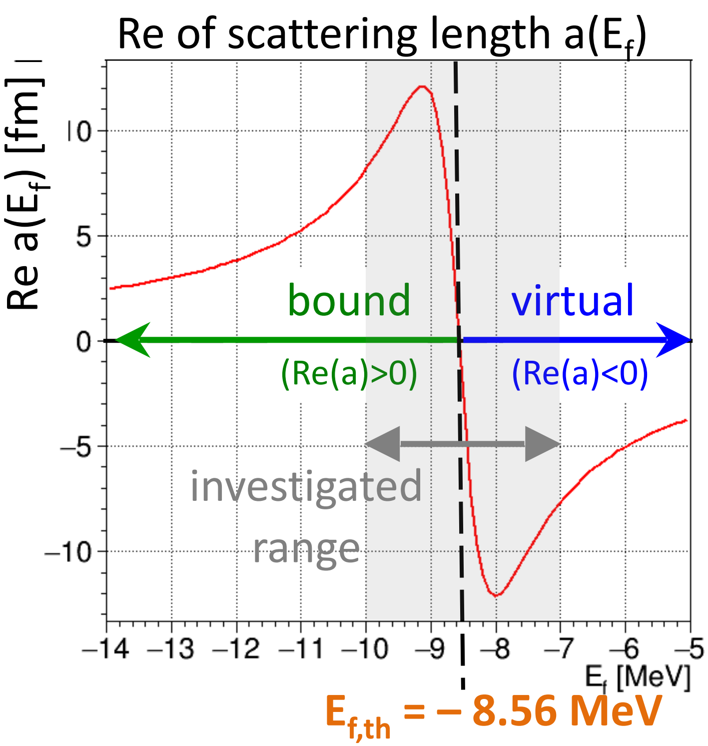

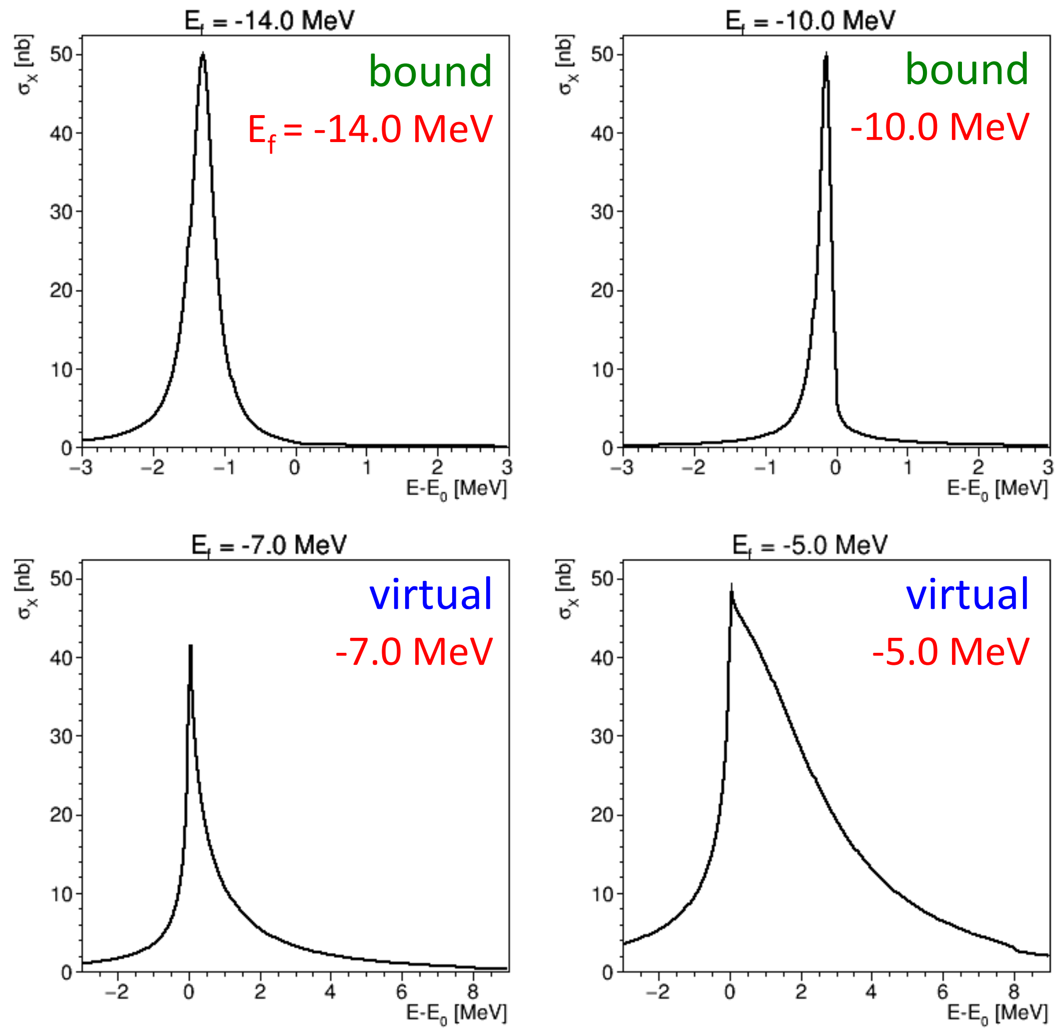

Klaus Goetzen, Frank Nerling, et al.

Sensitivity of PANDA

- Expected sensitivity for BW Width Γ & Flatté Parameter E_f
- Breit-Wigner: 3σ precision at down to Γ = O(50 − 100) keV!
- Flatté: Precision in sub-MeV range!

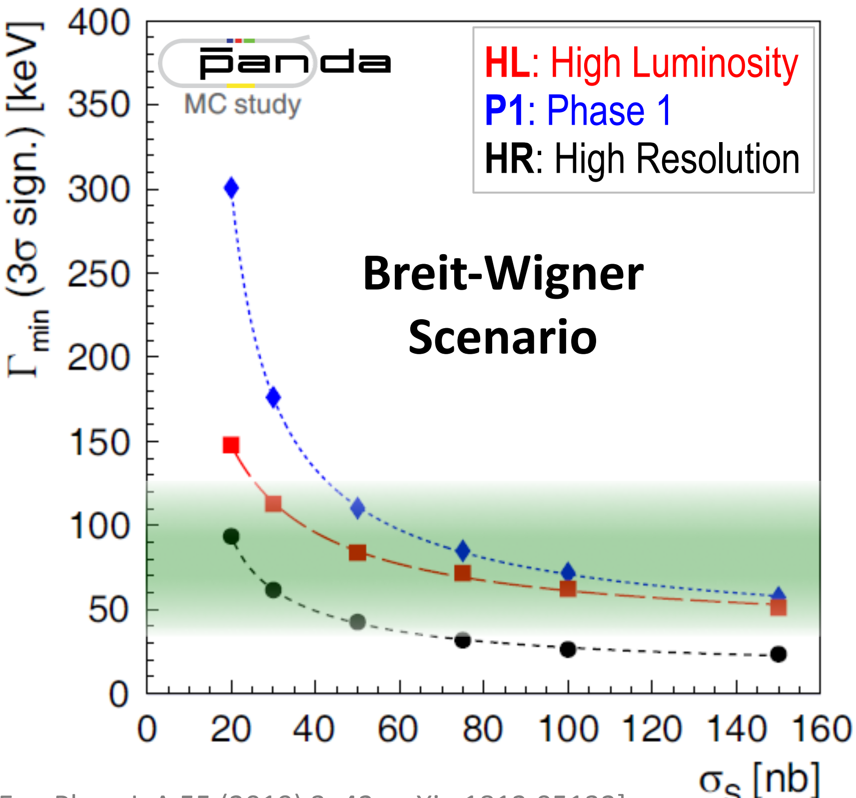

mis-id. bound → virtual state

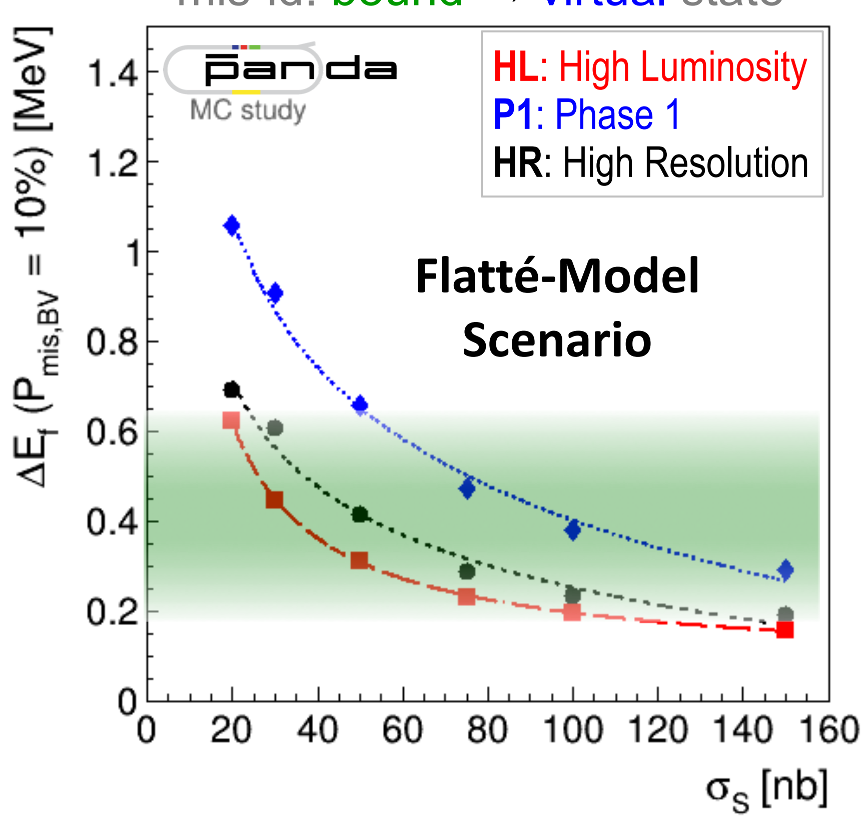

[Eur. Phys. J. A 55 (2019) 3, 42, arXiv:1812.05132]

Recent line-shape study of the X(3872)

[Phys.Rev.D 102 (2020) 9, 092005]
[https://arxiv.org/abs/2005.13419]

CERN-EP-2020-086
LHCb-PAPER-2020-008
May 27, 2020

Study of the lineshape of the $\chi_{c1}(3872)$ state

Abstract

A study of the lineshape of the $\chi_{c1}(3872)$ state is made using a data sample corresponding to an integrated luminosity of $3\,\text{fb}^{-1}$ collected in pp collisions at centre-of-mass energies of 7 and 8 TeV with the LHCb detector. Candidate $\chi_{c1}(3872)$ mesons from b-hadron decays are selected in the $J/\psi\pi^+\pi^-$ decay mode. Describing the lineshape with a Breit–Wigner function, the mass splitting between the $\chi_{c1}(3872)$ and $\psi(2S)$ states, Δm, and the width of the $\chi_{c1}(3872)$ state, Γ_{BW}, are determined to be

$$\begin{aligned} \Delta m &= 185.588 \pm 0.067 \pm 0.068\,\text{MeV}\,, \\ \Gamma_{\text{BW}} &= 1.39 \pm 0.24 \pm 0.10\,\text{MeV}\,, \end{aligned}$$

where the first uncertainty is statistical and the second systematic. Using a Flatté-inspired lineshape, two poles for the $\chi_{c1}(3872)$ state in the complex energy plane are found. The dominant pole is compatible with a quasi-bound $D^0\overline{D}^{*0}$ state but a quasi-virtual state is still allowed at the level of 2 standard deviations.

Recent line-shape study of the X(3872)

[Phys.Rev.D 102 (2020) 9, 092005]
[https://arxiv.org/abs/2005.13419]

CERN-EP-2020-086
LHCb-PAPER-2020-008
May 27, 2020

Study of the lineshape of the $\chi_{c1}(3872)$ state

Abstract

A study of the lineshape of the $\chi_{c1}(3872)$ state is made using a data sample corresponding to an integrated luminosity of $3\,\mathrm{fb}^{-1}$ collected in pp collisions at centre-of-mass energies of 7 and 8 TeV with the LHCb detector. Candidate $\chi_{c1}(3872)$ mesons from b-hadron decays are selected in the $J/\psi\pi^+\pi^-$ decay mode. Describing the lineshape with a Breit–Wigner function, the mass splitting between the $\chi_{c1}(3872)$ and $\psi(2S)$ states, Δm, and the width of the $\chi_{c1}(3872)$ state, Γ_{BW}, are determined to be

$$\begin{aligned}\Delta m &= 185.588 \pm 0.067 \pm 0.068\,\mathrm{MeV}\,,\\ \Gamma_{\mathrm{BW}} &= 1.39 \pm 0.24 \pm 0.10\,\mathrm{MeV}\,,\end{aligned}$$

where the first uncertainty is statistical and the second systematic. Using a Flatté-inspired lineshape, two poles for the $\chi_{c1}(3872)$ state in the complex energy plane are found. The dominant pole is compatible with a quasi-bound $D^0\overline{D}^{*0}$ state but a quasi-virtual state is still allowed at the level of 2 standard deviations.

Line-shape of the X(3872) - LHCb result

- Breit Wigner fit

$$m_{\chi_{c1}(3872)} = 3871.695 \pm 0.067 \pm 0.068 \pm 0.010\,\mathrm{MeV}$$

$$\Gamma_{BW} = 1.39 \pm 0.24 \pm 0.10\ \mathrm{MeV}$$

[previous Belle result: Γ < 1.2 MeV (CL90)]

[Phys.Rev.D 102 (2020) 9, 092005]
[https://arxiv.org/abs/2005.13419]

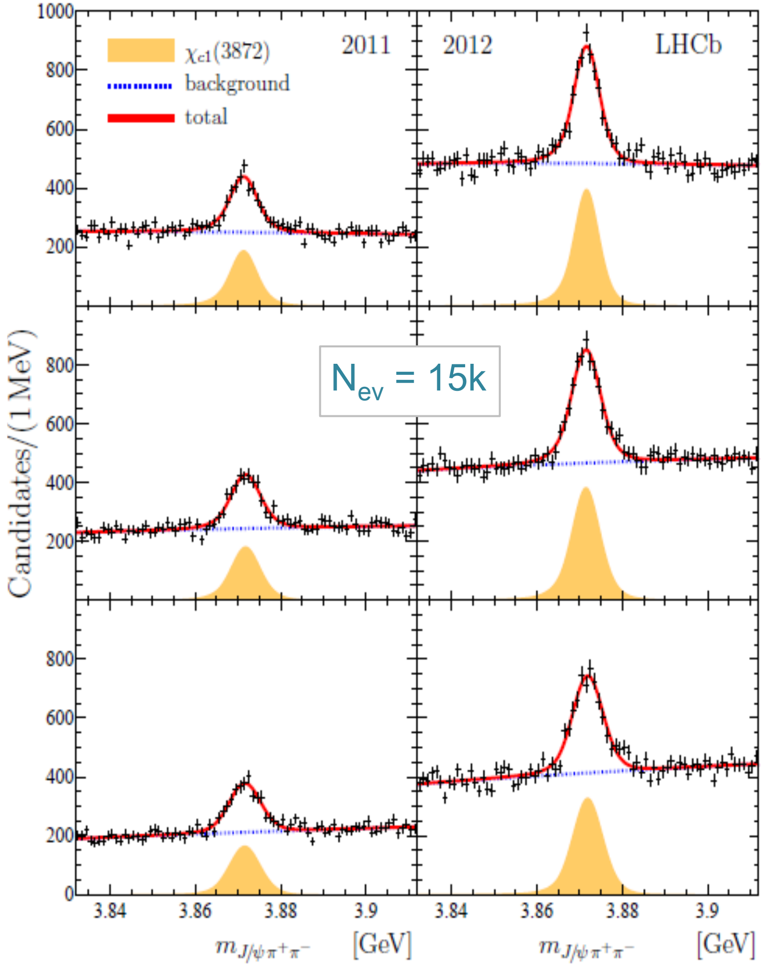

Line-shape of the X(3872) - LHCb result

- Breit Wigner fit

$$m_{\chi_{c1}(3872)} = 3871.695 \pm 0.067 \pm 0.068 \pm 0.010\,\text{MeV}$$
$$\Gamma_{\text{BW}} = 1.39 \pm 0.24 \pm 0.10\ \text{MeV}$$

[previous Belle result: Γ < 1.2 MeV (CL90)]

[Phys.Rev.D 102 (2020) 9, 092005]
[https://arxiv.org/abs/2005.13419]

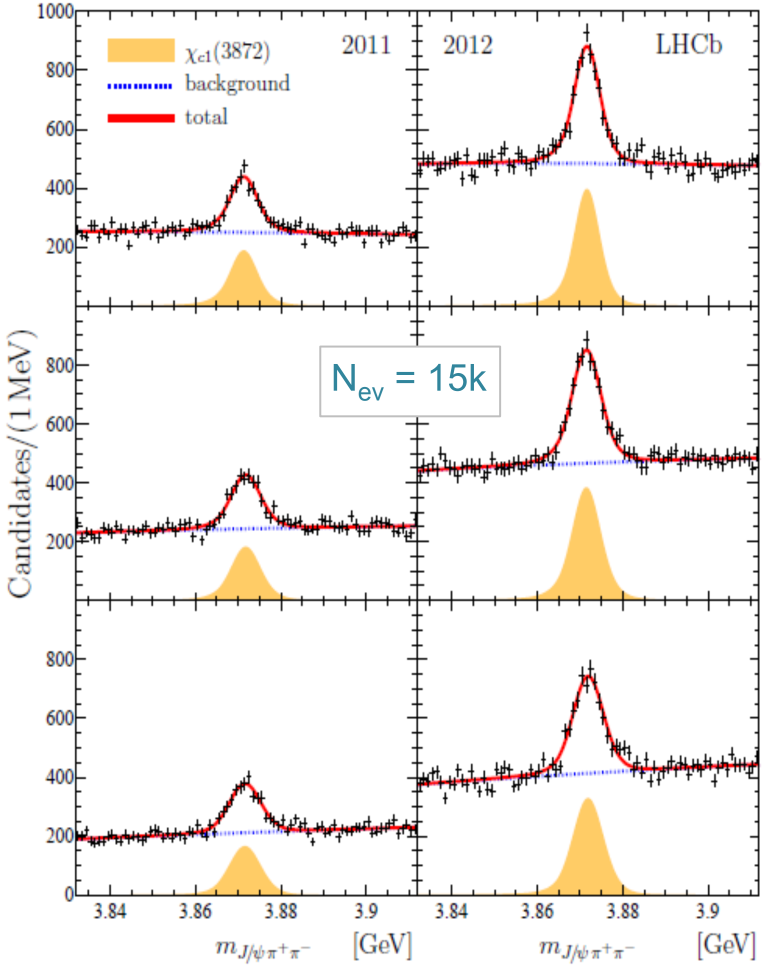

- Alternative Flatté model fit

Mode [MeV]	Mean [MeV]	FWHM [MeV]
$3871.69^{+0.00+0.05}_{-0.04-0.13}$	$3871.66^{+0.07+0.11}_{-0.06-0.13}$	$0.22^{+0.06+0.25}_{-0.08-0.17}$

g	$f_\rho \times 10^3$	Γ_0 [MeV]	m_0 [MeV]
0.108 ± 0.003	1.8 ± 0.6	1.4 ± 0.4	3864.5 (fixed)

(Flatté energy E_f = -7.2 MeV)

Line-shape of the X(3872) - LHCb result

- Breit Wigner fit

$$m_{\chi_{c1}(3872)} = 3871.695 \pm 0.067 \pm 0.068 \pm 0.010\,\mathrm{MeV}$$

$$\Gamma_{\mathrm{BW}} = 1.39 \pm 0.24 \pm 0.10\ \mathrm{MeV}$$

[previous Belle result: Γ < 1.2 MeV (CL90)]

[Phys.Rev.D 102 (2020) 9, 092005]
[https://arxiv.org/abs/2005.13419]

Factor 6.3, analysis dependent

- Alternative Flatté model fit

Mode [MeV]	Mean [MeV]	FWHM [MeV]
$3871.69^{+0.00+0.05}_{-0.04-0.13}$	$3871.66^{+0.07+0.11}_{-0.06-0.13}$	$0.22^{+0.06+0.25}_{-0.08-0.17}$

g	$f_\rho \times 10^3$	Γ_0 [MeV]	m_0 [MeV]
0.108 ± 0.003	1.8 ± 0.6	1.4 ± 0.4	3864.5 (fixed)

(Flatté energy E_f = -7.2 MeV)

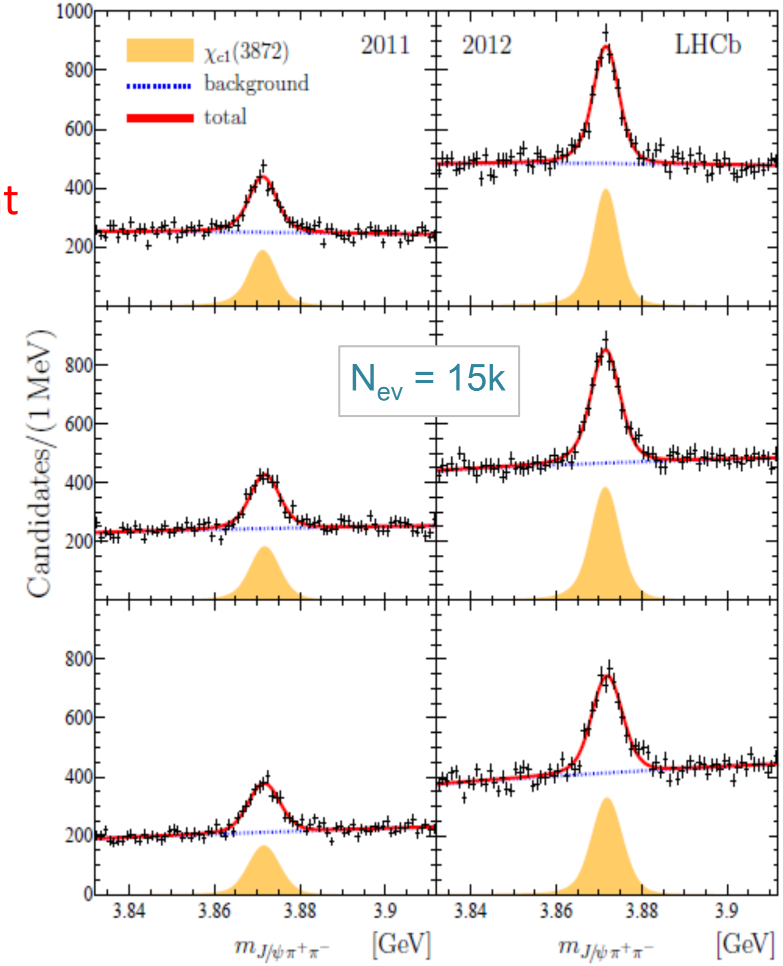

Line-shape of the X(3872) - LHCb result

- Breit Wigner fit

$$m_{\chi_{c1}(3872)} = 3871.695 \pm 0.067 \pm 0.068 \pm 0.010\,\mathrm{MeV}$$

$$\Gamma_{\mathrm{BW}} = 1.39 \pm 0.24 \pm 0.10\ \mathrm{MeV}$$

[previous Belle result: Γ < 1.2 MeV (CL90)]

[Phys.Rev.D 102 (2020) 9, 092005]
[https://arxiv.org/abs/2005.13419]

Factor 6.3, analysis dependent

- Alternative Flatté model fit

Mode [MeV]	Mean [MeV]	FWHM [MeV]
$3871.69^{+0.00+0.05}_{-0.04-0.13}$	$3871.66^{+0.07+0.11}_{-0.06-0.13}$	$0.22^{+0.06+0.25}_{-0.08-0.17}$

g	$f_\rho \times 10^3$	Γ_0 [MeV]	m_0 [MeV]
0.108 ± 0.003	1.8 ± 0.6	1.4 ± 0.4	3864.5 (fixed)

(Flatté energy E_f = -7.2 MeV)

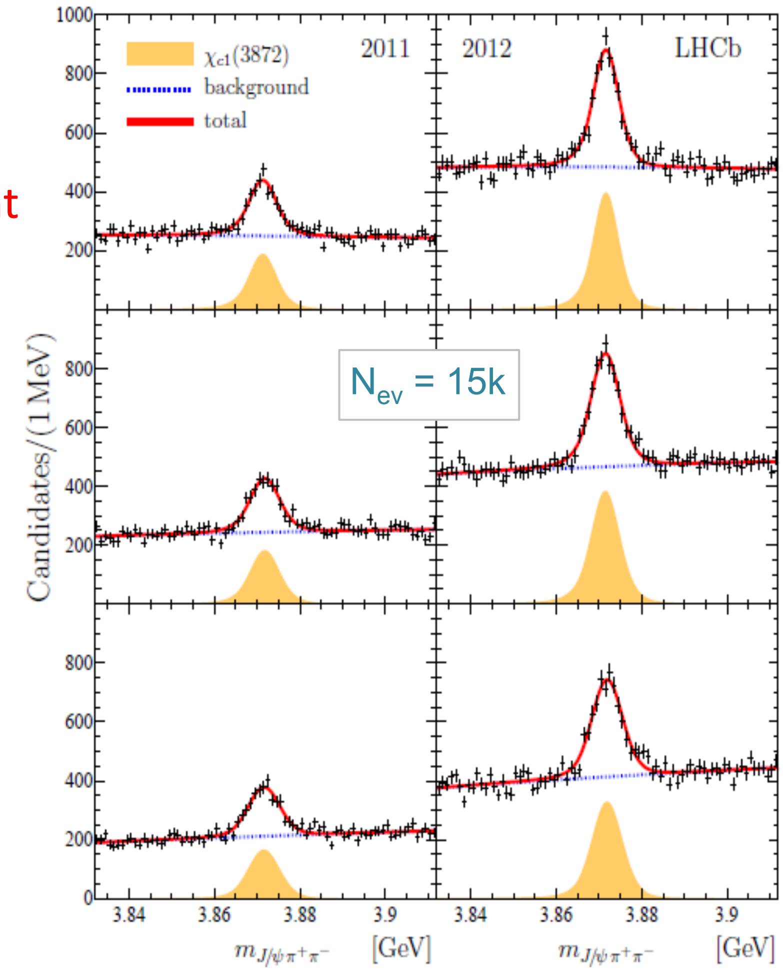

→ Conclusion depends on the model!

Line-shape of the X(3872) - LHCb vs PANDA

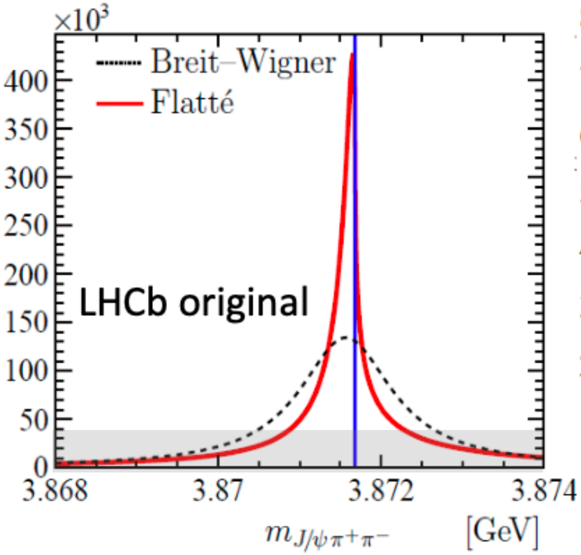

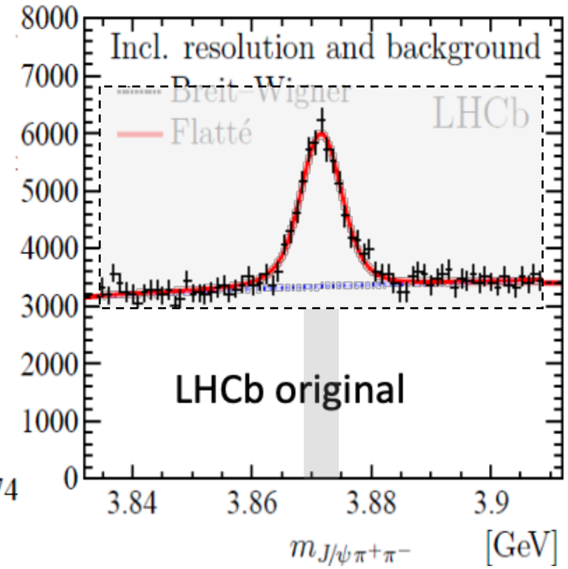

- Width assuming **B-W**:
  $\Gamma = 1.39 \mp 0.24 \mp 0.10$ MeV (LHCb 2020*)
- Width assuming **Flatté** model:
  FWHM = $0.22^{+0.06+0.25}_{-0.08-0.17}$ MeV (LHCb 2020*))

→ Not possible to distinguish by LHCb

* LHCb: Phys. Rev. D 102, 9, 092005 (2020)

Line-shape of the X(3872) - LHCb vs PANDA

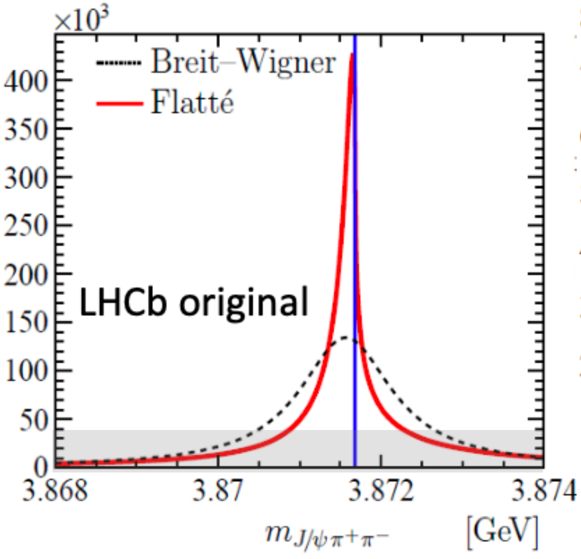

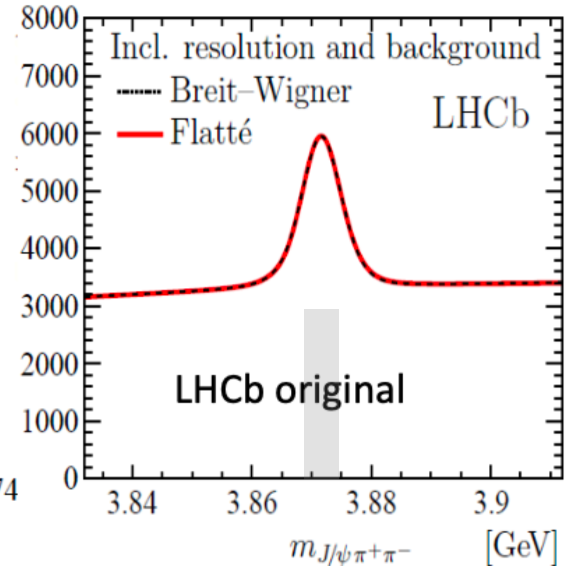

- Width assuming **B-W**:
  $\Gamma = 1.39 \mp 0.24 \mp 0.10$ MeV (LHCb 2020*)
- Width assuming **Flatté** model:
  FWHM = $0.22^{+0.06+0.25}_{-0.08-0.17}$ MeV (LHCb 2020*))

→ Not possible to distinguish by LHCb

* LHCb: Phys. Rev. D 102, 9, 092005 (2020)

Line-shape of the X(3872) - LHCb vs PANDA

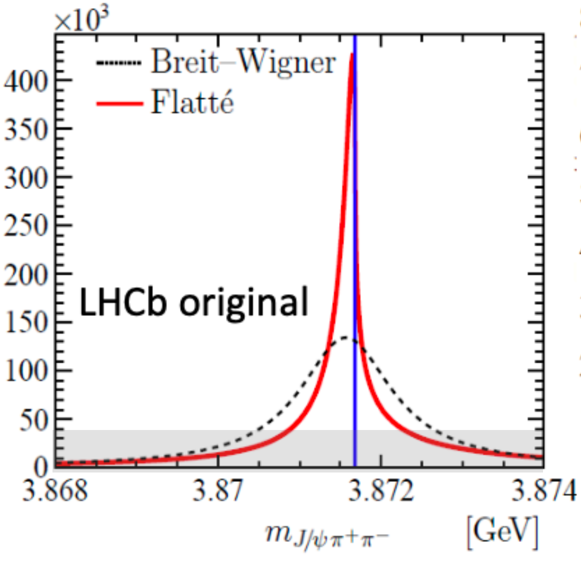

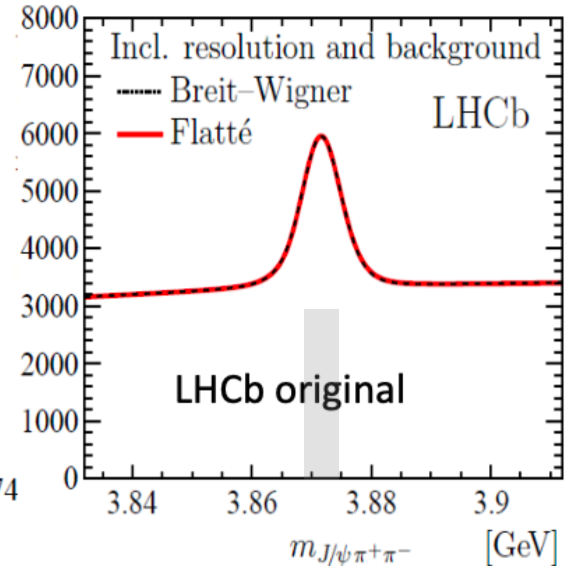

- Width assuming **B-W**:
  $\Gamma = 1.39 \mp 0.24 \mp 0.10$ MeV (LHCb 2020*)
- Width assuming **Flatté** model:
  FWHM = $0.22^{+0.06+0.25}_{-0.08-0.17}$ MeV (LHCb 2020*))

→ Not possible to distinguish by LHCb

* LHCb: Phys. Rev. D 102, 9, 092005 (2020)

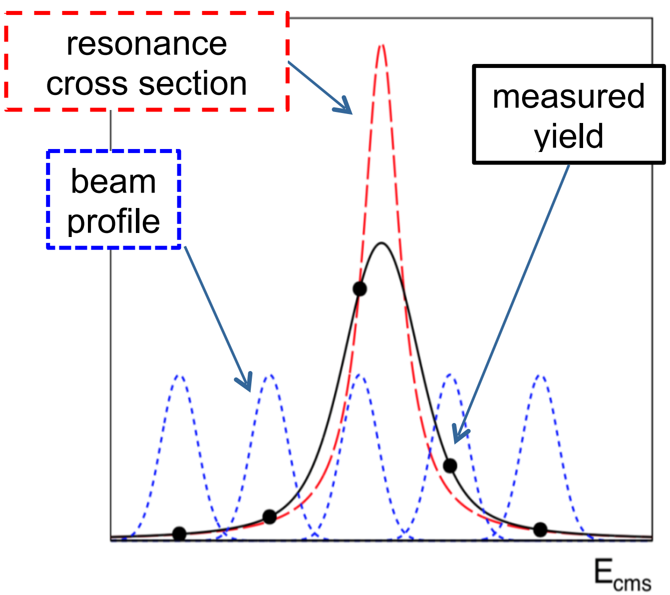

Line-shape of the X(3872) - LHCb vs PANDA

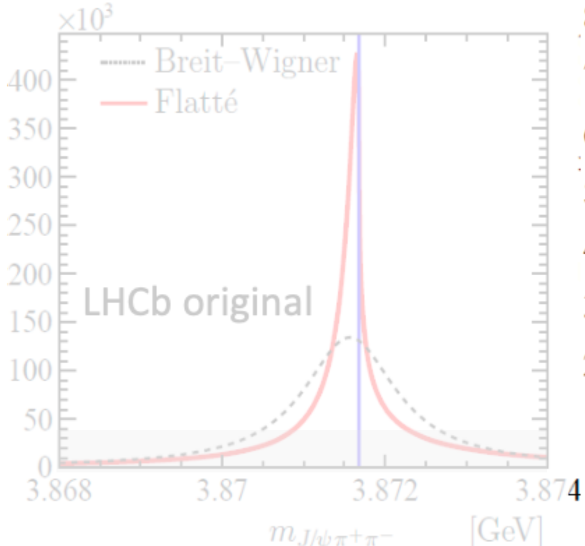

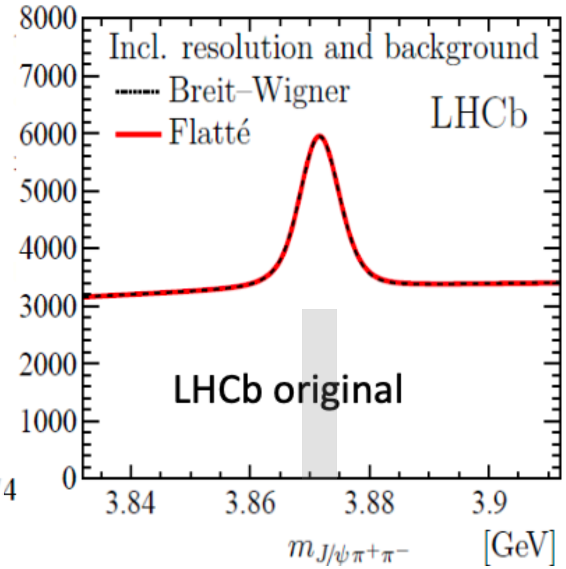

- Width assuming **B-W**:
  $\Gamma = 1.39 \mp 0.24 \mp 0.10$ MeV (LHCb 2020*)
- Width assuming **Flatté** model:
  FWHM = $0.22^{+0.06+0.25}_{-0.08-0.17}$ MeV (LHCb 2020*))

→ Not possible to distinguish by LHCb

* LHCb: Phys. Rev. D 102, 9, 092005 (2020)

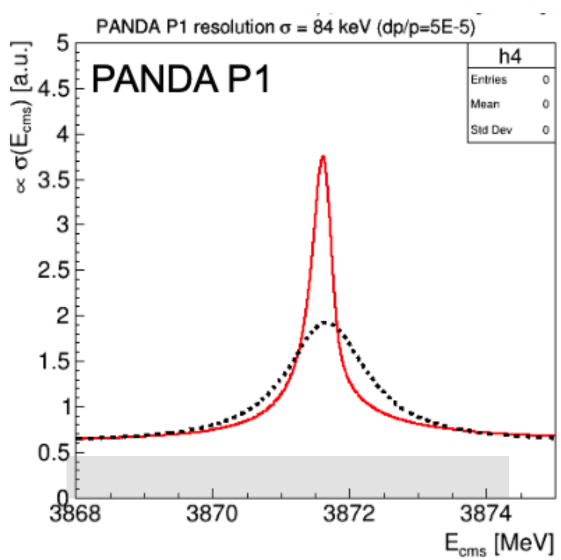

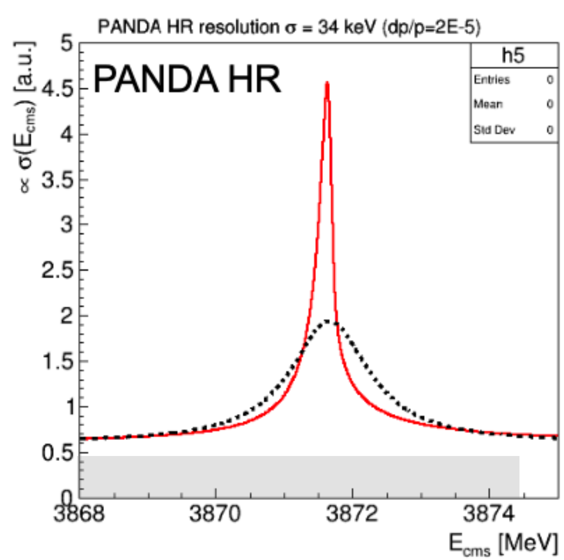

MC simulation - Flatte vs BW

We use the following approach:

1. Use key parameters from EPJ A 55 (2019) 42
2. Generate many spectra for Flatté (BW) model
3. Fit both BW and Flatté to each generated distribution and determine fit probabilities P_{BW} and P_F
4. Identification considered correct, if $P_F > P_{BW}$ ($P_{BW} > P_F$)
5. Count fraction of incorrect assignments → P_{mis}
6. P_{mis} measure for separation power
7. P_{mis} = 50% means: models indistinguishable

MC simulation - Flatte vs BW

Performance across Flatté energy E_f range

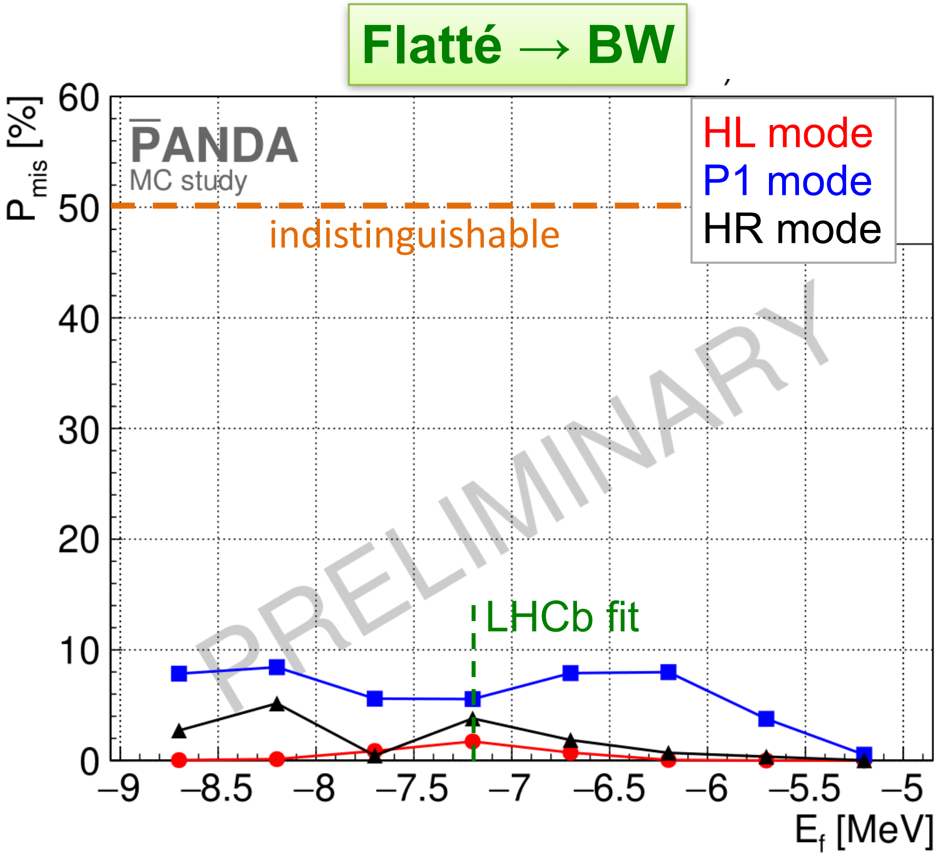

For Mis-match of Flatté as BW we see

- for the three beam modes **HL**, **HR**, **P1**
- the mis-identification probability $\mathbf{P_{mis}}$
- across range of input parameters $\mathbf{E_f}$
- with **LHCb** best fit E_f = -7.2 MeV
- and $\mathbf{P_{mis}}$ **= 50%** for "indistinguishable"

MC simulation - Flatte vs BW

Performance across Flatté energy E_f / Breit-Wigner Γ range

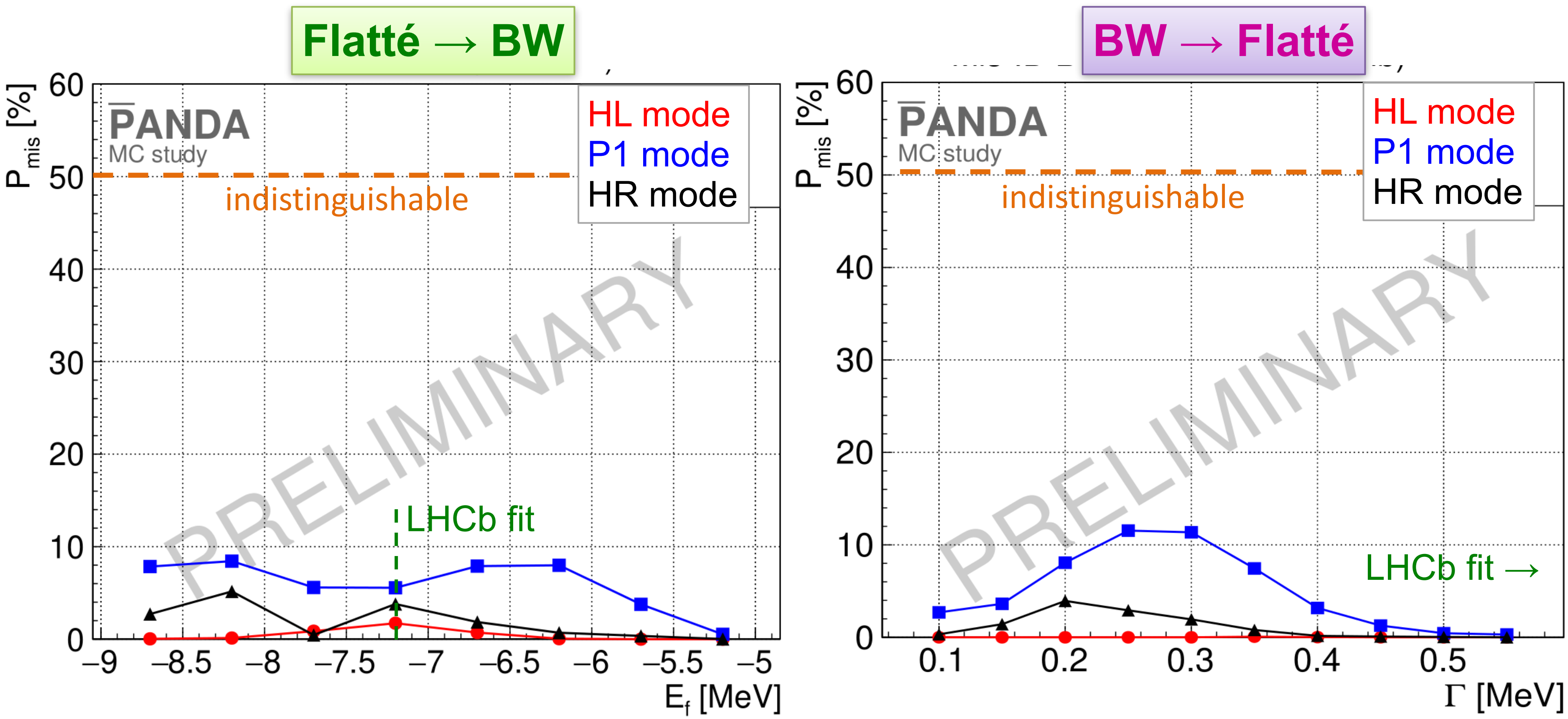

K.Götzen & F.Nerling, for PANDA, XYZ workshop at GSI, April 2021; F.Nerling, for PANDA, PoS(CHARM2020)004, May 2021

MC simulation - Flatte vs BW

Performance across Flatté energy E_f / Breit-Wigner Γ range

Flatté → BW

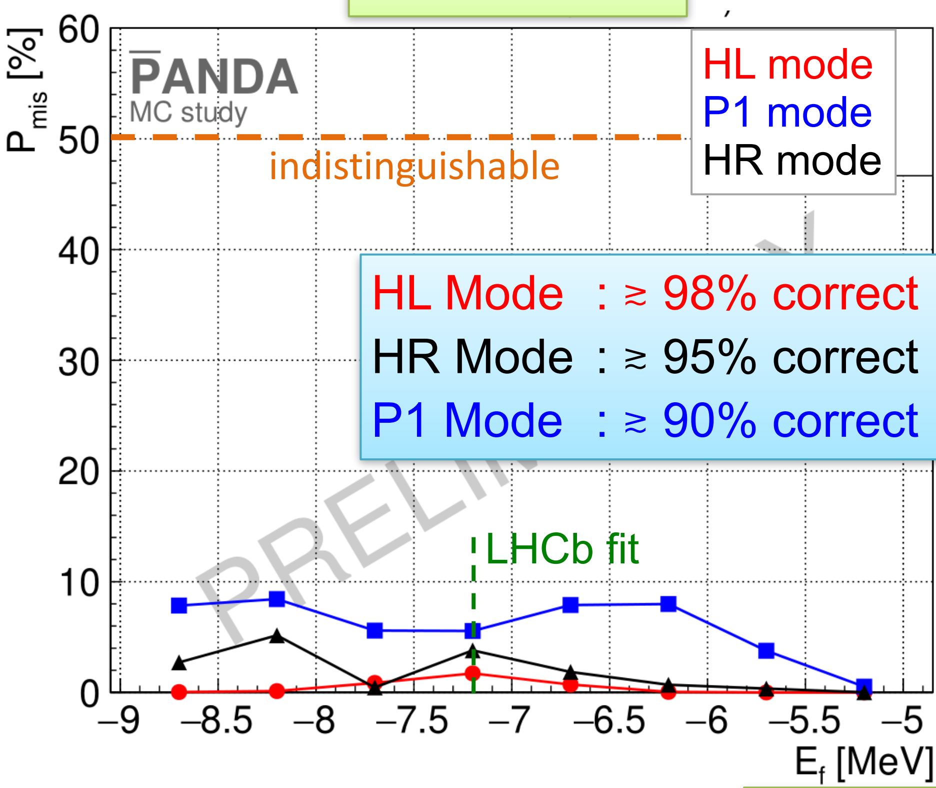

BW → Flatté

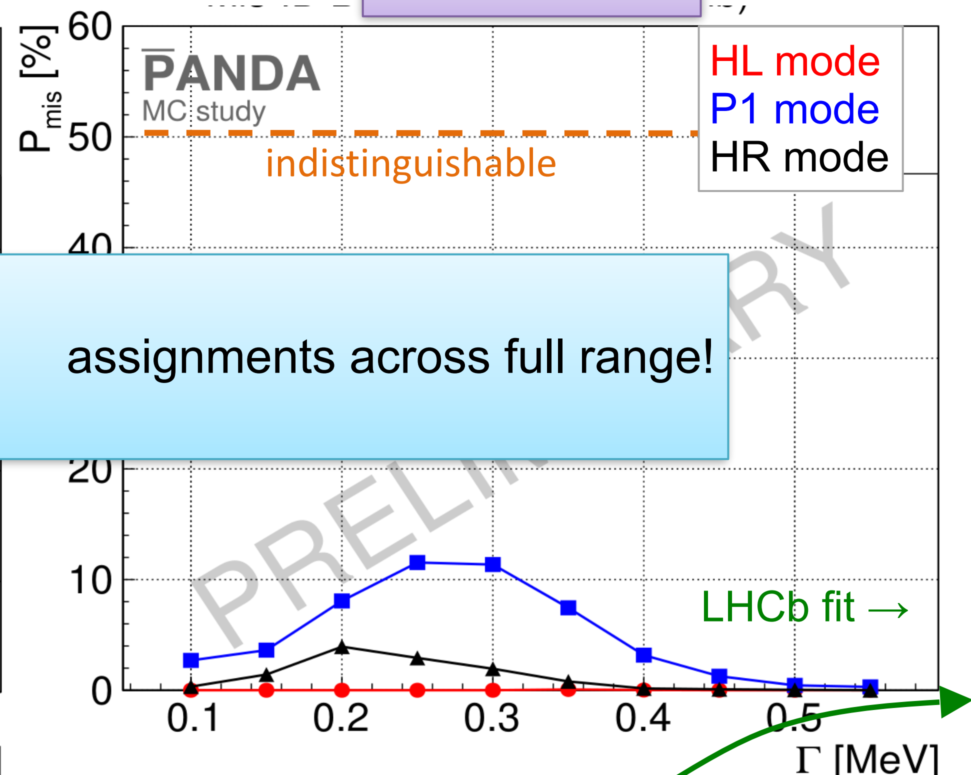

HL Mode : ≳ 98% correct
HR Mode : ≳ 95% correct
P1 Mode : ≳ 90% correct
assignments across full range!

N.B.: For BW **Γ = 1.4 MeV** we find 0% mis-ID in all modes...

K.Götzen & F.Nerling, for PANDA, XYZ workshop at GSI, April 2021; F.Nerling, for PANDA, PoS(CHARM2020)004, May 2021

Heavy Quarkonium Spectroscopy with PANDA

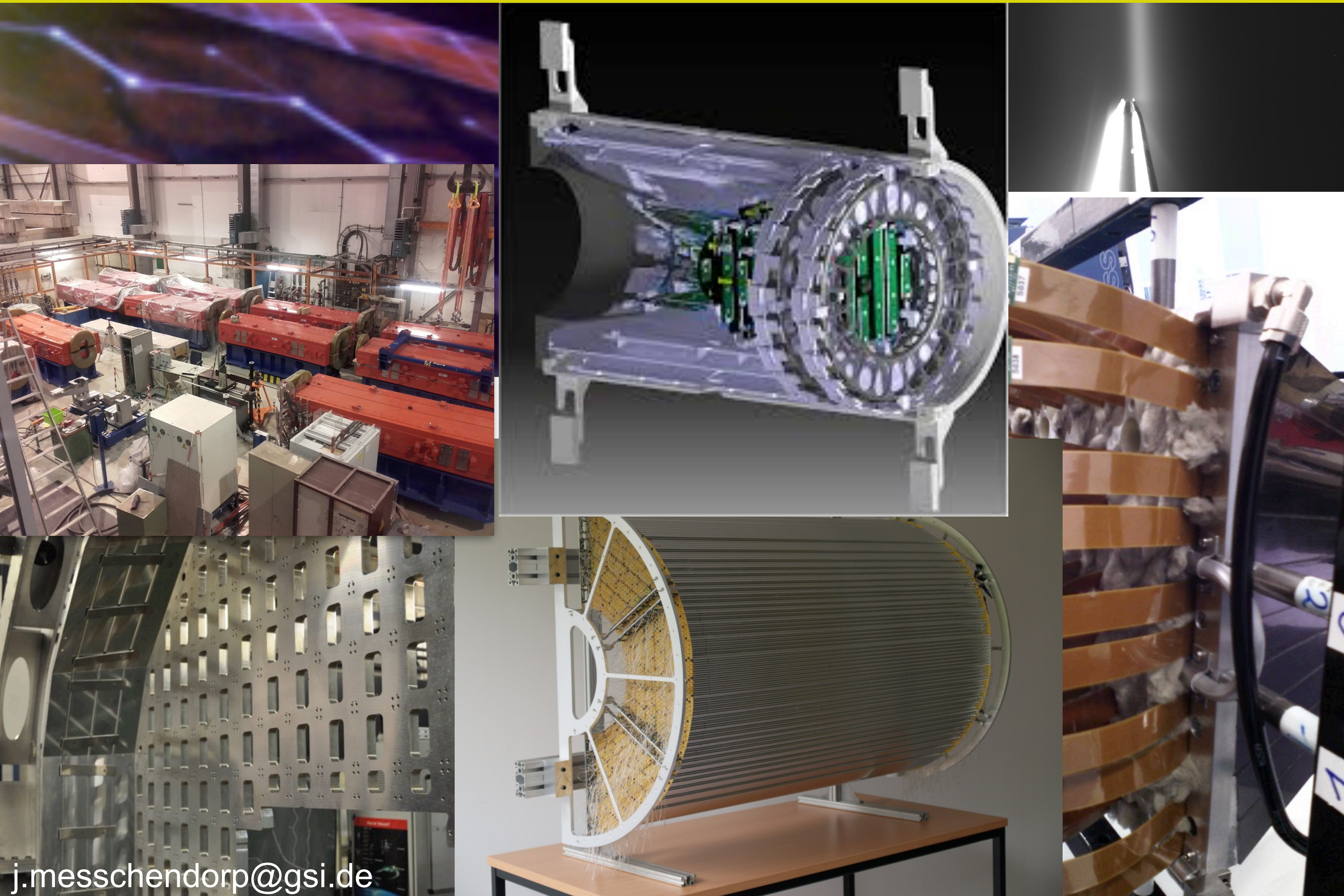

j.messchendorp@gsi.de

Heavy Quarkonium Spectroscopy with PANDA

… PANDA remains a key pillar at FAIR
- ESFRI landmark, top priority NuPECC
- civil construction of FAIR well underway
- presently under ‘scientific' review

… with a strong *spectroscopy* program
- glueballs, (hidden)charm, strangeness baryons, …
- discovery by large coverage in J^{PC}
- conclusive via precision, *e.g.* resonance scanning

… is complementary and competitive
- *unique* antiproton facility

… remains vigilant (and patient)

j.messchendorp@gsi.de

Backup

Demo

Klaus Goetzen, Frank Nerling, et al.

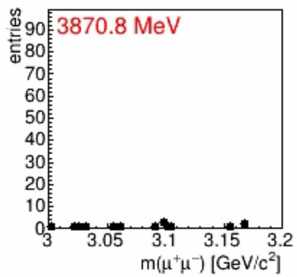

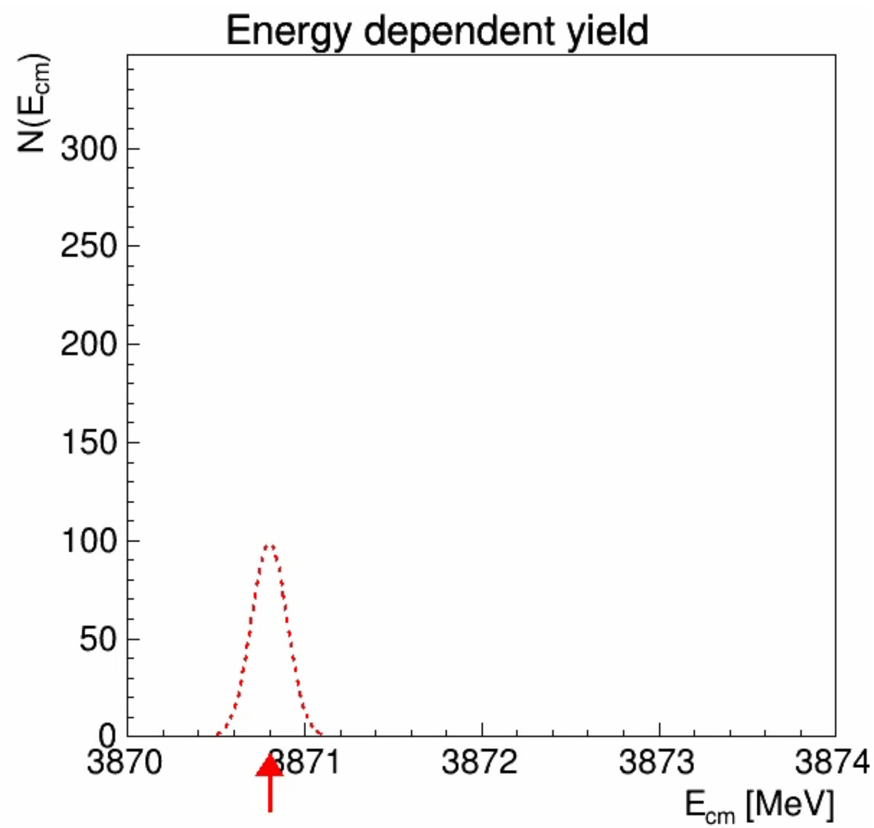

Demo

Klaus Goetzen, Frank Nerling, et al.

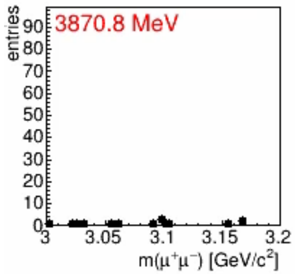

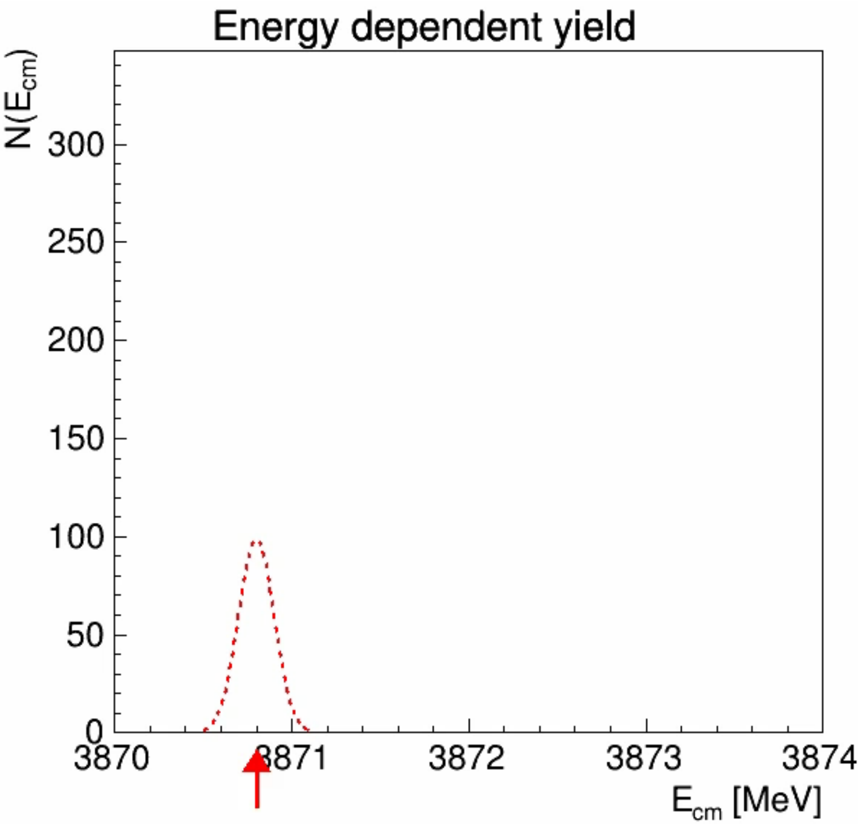

Demo

Klaus Goetzen, Frank Nerling, et al.

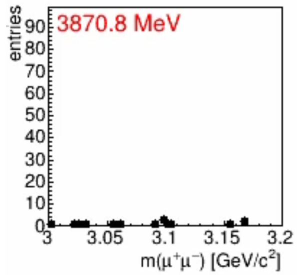

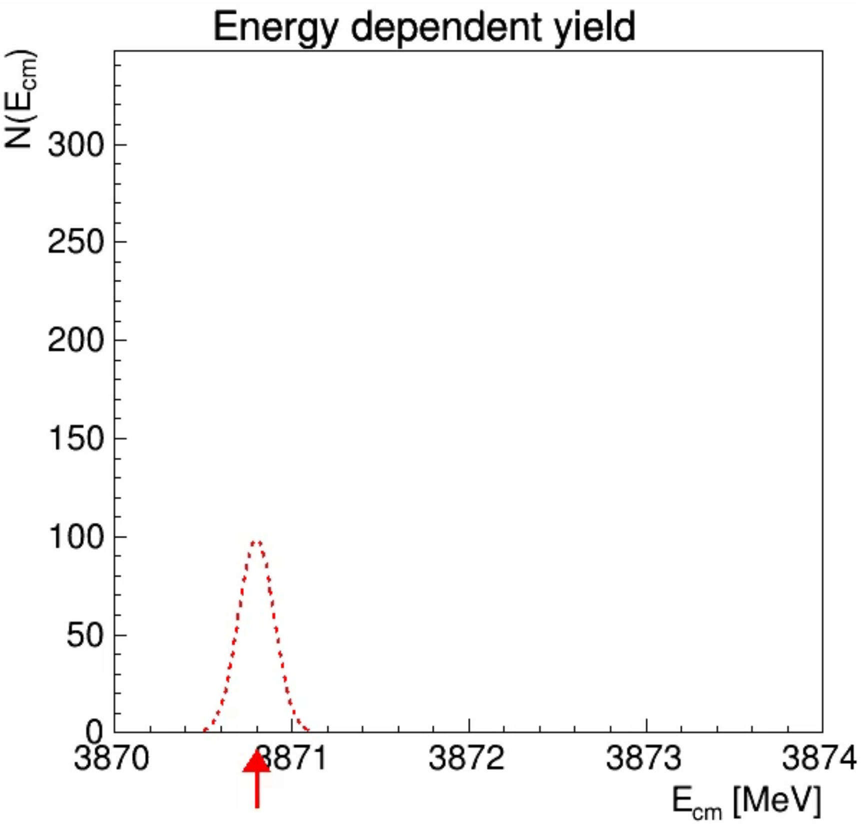

Flatté Model (Hanhart et al.)

[PRD 76 (2007) 034007]

$$\frac{dBr(B \to KD^0\bar{D}^{*0})}{dE} = \mathcal{B}\frac{1}{2\pi}\frac{gk_1}{|D(E)|^2},$$

$$\frac{dBr(B \to K\pi^+\pi^- J/\psi)}{dE} = \mathcal{B}\frac{1}{2\pi}\frac{\Gamma_{\pi^+\pi^- J/\psi}(E)}{|D(E)|^2},$$

J/ψπ+π– lineshape

with

Flatté Energy

$$D(E) = \begin{cases} E - E_f - \frac{g_1\kappa_1}{2} - \frac{g_2\kappa_2}{2} + i\frac{\Gamma(E)}{2}, & E < 0 \\ E - E_f - \frac{g_2\kappa_2}{2} + i\left(\frac{g_1k_1}{2} + \frac{\Gamma(E)}{2}\right), & 0 < E < \delta \\ E - E_f + i\left(\frac{g_1k_1}{2} + \frac{g_2k_2}{2} + \frac{\Gamma(E)}{2}\right), & E > \delta \end{cases}$$

$$k_1 = \sqrt{2\mu_1 E}, \qquad \mu_1 = \frac{m_{D^0}m_{D^{*0}}}{(m_{D^0}+m_{D^{*0}})}$$

$$\kappa_1 = \sqrt{-2\mu_1 E}, \qquad \mu_2 = \frac{m_{D^+}m_{D^{*-}}}{(m_{D^+}+m_{D^{*-}})}$$

$$k_2 = \sqrt{2\mu_2(E-\delta)}, \qquad \delta = 8.2\,\text{MeV}$$

$$\kappa_2 = \sqrt{2\mu_2(\delta - E)}$$

$$g_1 = g_2 = g$$

$$E_{f,thr} = -g\sqrt{\mu_2\delta/2}$$

threshold bound/virtual

$$\Gamma(E) = \Gamma_{\pi^+\pi^- J/\psi}(E) + \Gamma_{\pi^+\pi^-\pi^0 J/\psi}(E) + \Gamma_0,$$

$$\Gamma_{\pi^+\pi^- J/\psi}(E) = f_\rho \int_{2m_\pi}^{M-m_{J/\psi}} \frac{dm}{2\pi}\frac{q(m)\Gamma_\rho}{(m-m_\rho)^2 + \Gamma_\rho^2/4},$$

$$\Gamma_{\pi^+\pi^-\pi^0 J/\psi}(E) = f_\omega \int_{3m_\pi}^{M-m_{J/\psi}} \frac{dm}{2\pi}\frac{q(m)\Gamma_\omega}{(m-m_\omega)^2 + \Gamma_\omega^2/4},$$

Param.	EPJ A 55 42 (PANDA, 2019)	PRD 102 092005 (LHCb, 2020)
g	0.137	0.108
Γ_0	1.0 MeV	1.4 MeV
f_ρ	0.007	0.0018
f_ω	0.036	0.01
E_f	*study range*	-7.2 MeV
$E_{f,thr}$	-8.56 MeV	-6.82 MeV

Key Parameters from EPJ A 55 (2019) 42

Reconstruction of: ⍰p $\rightarrow \chi_{c1}(3872) \rightarrow J/\psi\ (\rightarrow e^+e^- / \mu^+\mu^-)\ \rho^0\ (\rightarrow \pi^+\pi^-)$

Category	Parameter	Value
Reco Efficiencies	Signal (average $J/\psi \rightarrow e^+ e^-$ and $J/\psi \rightarrow \mu^+ \mu^-$)	13.7 %
	Non-resonant background (")	2.9 %
	⍰p → multi-hadron background	$2.8 \cdot 10^{-10}$
Branching fractions	$BR(J/\psi \rightarrow e^+e^-)$	5.97 %
	$BR(J/\psi \rightarrow \mu^+\mu^-)$	5.96 %
	$BR(\rho^0 \rightarrow \pi^+\pi^-)$	100 %
	$BR(X \rightarrow J/\psi\ \rho^0)$	5 %
Cross sections	σ_{peak}(⍰p → X)	[20,30,**50**,75,100,150] nb
	σ(⍰p → $J/\psi\ \pi^+\pi^-$ non-res)	1.2 nb [PRD 77 (2008) 097501]
	σ(⍰p → inelast.) @ 3.872 GeV	46 mb
Luminosity & Resolution	HL : L_{HL} / dE_{HL}	13680 $(nb \cdot d)^{-1}$ / 168 keV
	HR : L_{HR} / dE_{HR}	1370 $(nb \cdot d)^{-1}$ / 34 keV
	P1 : L_{P1} / dE_{P1}	1170 $(nb \cdot d)^{-1}$ / 84 keV
Scan time	T_{tot}	40 × 2d = 80d
Model Parameters	Breit Wigner Width Γ	[50, 70, 100, 130, 180, 250, 500] keV
	Flatté Model Energy E_f	- [10.0, 9.5, 9.0, 8.8, 8.3, 8.0, 7.5, 7.0] MeV

Production Cross Section Estimate $\chi_{c1}(3872)$

- Cross section $\sigma(\bar{p}p \rightarrow \chi_{c1}(3872))$ yet unknown
- Estimate from $\mathscr{B}(\chi_{c1}(3872) \rightarrow \bar{p}p)$ via crossing symmetry

$$\sigma_{i\rightarrow X}(M_X) = \frac{3 \bullet 4\pi}{M_X^2 - 4m_p^2} \bullet \mathscr{B}(X \rightarrow i) = 1.28\text{mb} \bullet \mathscr{B}(X \rightarrow i)$$

- Relevant publications

  a) Eur. Phys. J C73, 2462 (2013):

  Ɓ(X → p?) < 0.002 · Ɓ(X→J/ψ $\pi^+\pi^-$) with Ɓ(X→J/ψ $\pi^+\pi^-$) > 3.2%

  * using BR(X → J/ψππ) < [100% − sum of all other lower limits BR] = 20.9% as UL

  → σ(p? → X) ~ 81.9 nb **(< 535 nb*)**

  b) Phys. Lett. B 769 (2017) 305-313:

  Ɓ(B^+ → XK^+ → p?K^+) / Ɓ(B^+ → J/ψK^+→ p? K^+) < 0.002

  - with Ɓ(B^+ → J/ψK^+→ p?K^+) = $2.2\cdot10^{-6}$ and Ɓ(B^+ → XK^+) < $2.6\cdot10^{-4}$

    ** using BR(B^+ → XK^+) = $1.2\cdot10^{-4}$ from Belle paper PRD 97 (2018) 1, 012005

    → σ(p? → X) ~ 21.7 nb (**< 46.9 nb****)

  - with Ɓ(B^+ → XK^+→ ppK^+) < $5\cdot10^{-9}$

    → σ(p? → X) ~ 24.6 nb (**< 53.3 nb****)

- Using **σ(p? → X) = 50 nb** (default from our publication)

Perspectives with resonance scanning at PANDA

- Due to precise beam resolution
  → Breit-Wigner and Flatté-model are distinguishable

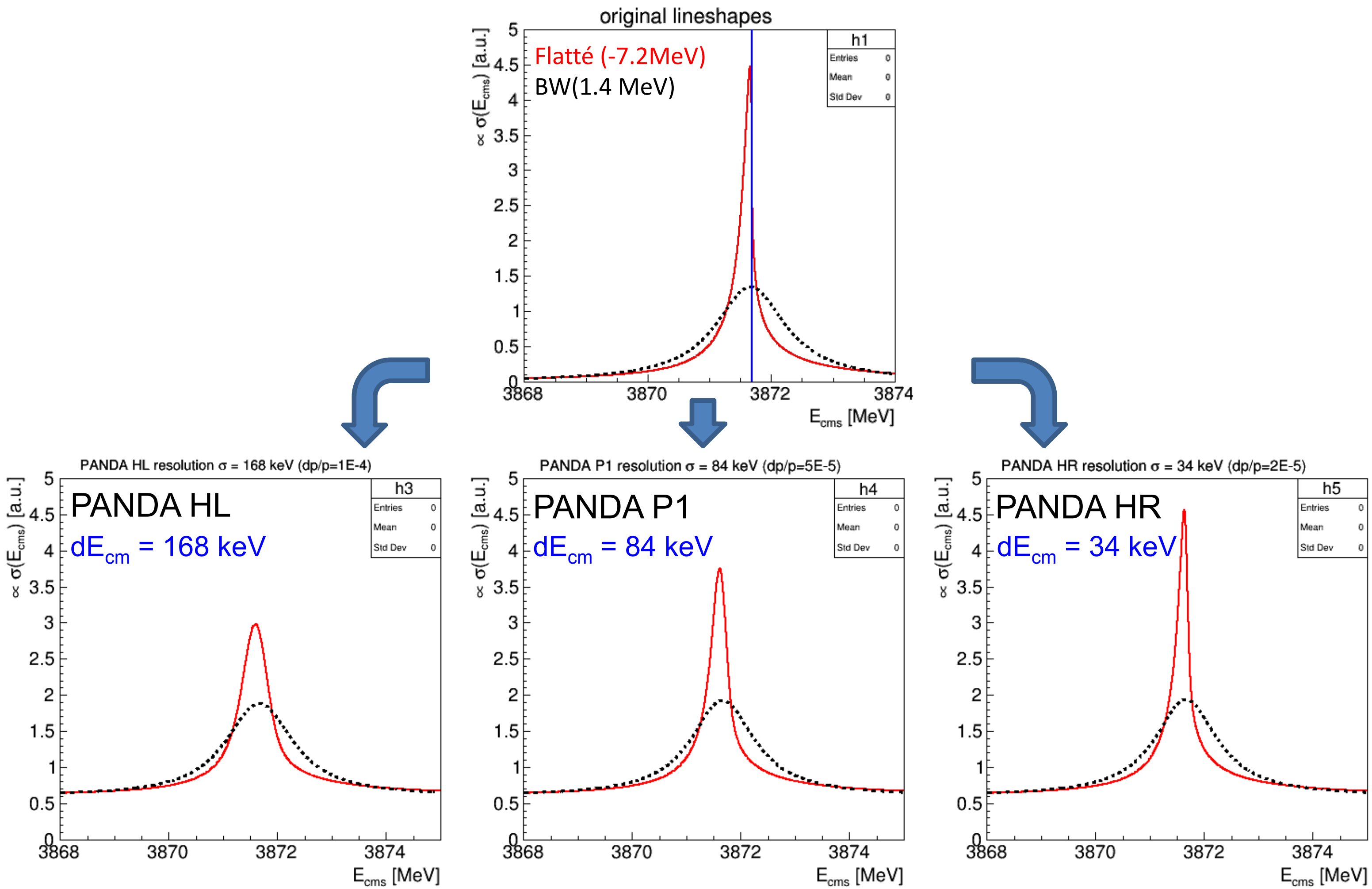

Distinction of Line Shapes (Param. E_f)

- Simulation study: Input $E_{f,0}$ → output distr. $E_{f,meas}$ (1000 fits)
- Idea: Estimate probability to mix up virtual and bound state
- Quantify by fraction of wrongly identified states

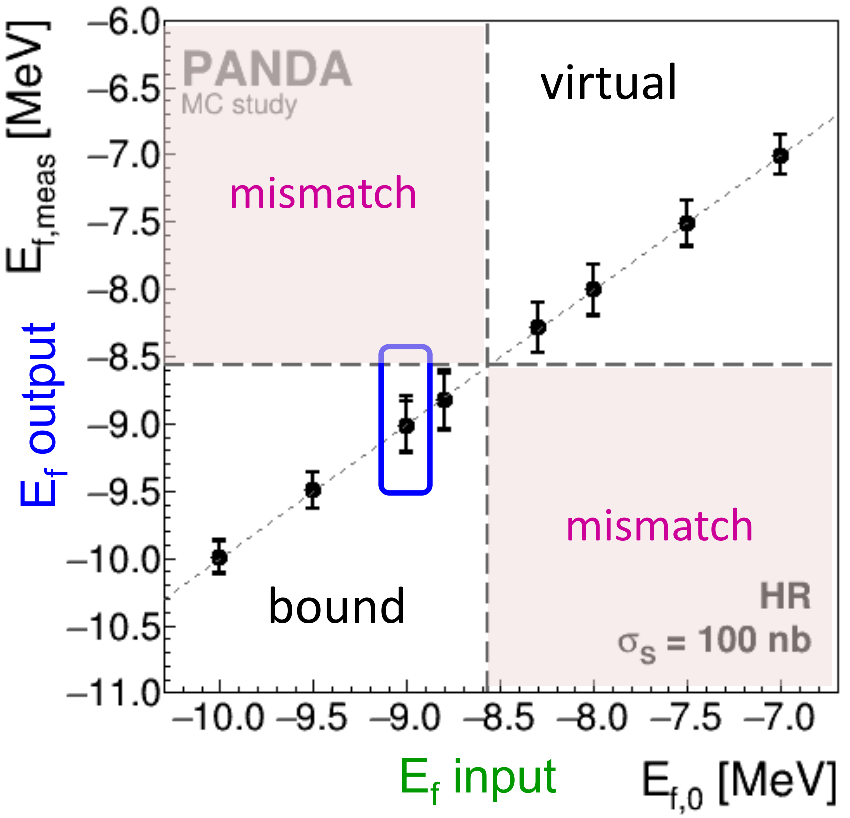

E_f output distribution

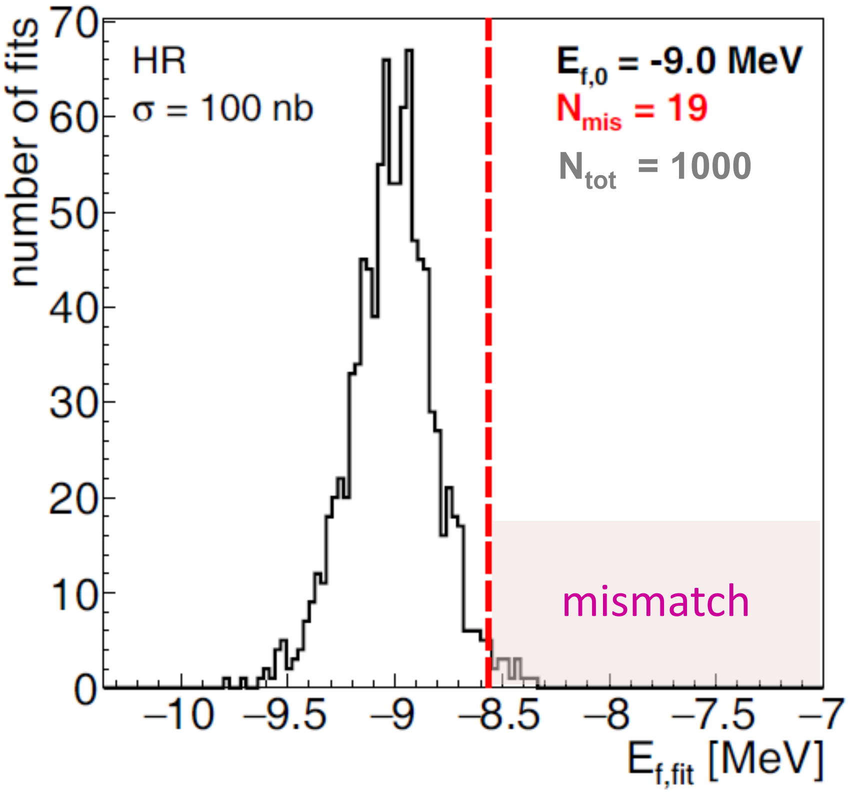

Distinction of Line Shapes E_f (condensed)

- Again: Condense to cross section dependent result
- Extract input $E_{f,0}$ where P_{mis} = 10% (90% correct identification)
- Enter $\Delta E_f = E_{f,0} - E_{f,thr}$ in cross section dependent graph

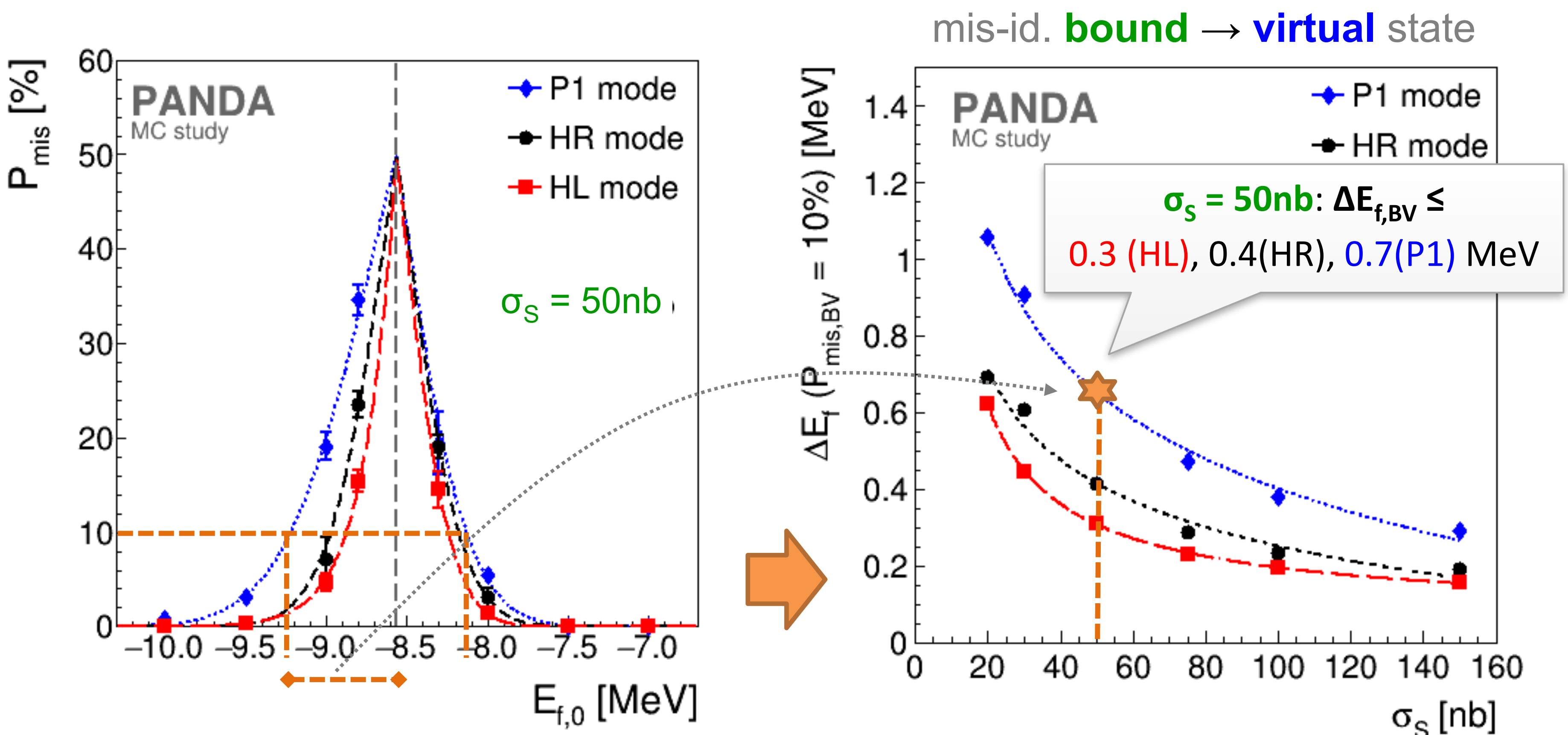

Distinction of Line Shapes E_f (condensed)

- Again: Condense to cross section dependent result
- Extract input $E_{f,0}$ where P_{mis} = 10% (90% correct identification)
- Enter $\Delta E_f = E_{f,0} - E_{f,thr}$ in cross section dependent graph